Deanship of Graduate Studies

Al-Quds University

X Chromosome Inactivation Patterns in Human Induced Pluripotent Stem Cells

Shatha Al.Eman Khaled Sawalha

M.Sc. Thesis

Jerusalem, Palestine

2018 م - 1439هـ

X Chromosome Inactivation Patterns in Human Induced Pluripotent Stem Cells (hiPSC)

Prepared by:

Shatha Al.Eman Khaled M.Sawalha

B.Sc. Biology, Al-Quds University, Palestine

Supervised by:

Prof. Zaidoun Salah **Prof. Mieke Geens**

This thesis is submitted in partial fulfillment of requirements for the degree of Master of Applied and Industrial Technology Program at Faculty of Science, Al-Quds University.

1439/2018

Al-Quds University

Deanship of Graduate Studies

Applied Industrial Technology Program

Thesis Approval

X Chromosome Inactivation Patterns in Human Induced Pluripotent Stem Cells (hiPSC)

Prepared by: Shatha Al.Eman Khaled Sawalha

Registration No.: 21512742

Supervisor: Prof. Zaidoun Salah
Co-Supervisor: Prof.Mieke Geens

Master thesis Submitted and Accepted, Date 3/6/2018

The names and signatures of the examining committee members are as follows:

1-Head of Committee/ Prof.Zaidoun Salah Signature:.....

2- Internal Examiner/ Dr.Omar Hamarsheh Signature:.....

3- External Examiner/Dr. Suheir Eriqat Signature: .....

Jerusalem–Palestine
1439/2018

Dedication

I would like to dedicate this thesis to my beloved parents, Khaled and Hend, who have always lighten my road up to seek science constantly and give me power to keep on,

To my sisters and brothers ,Noor, Maryam, Ruba, Yafa, Kareem, Mohammed ,and Limar for who never stop giving themselves in countless ways,

To all my supportive friends during this journey,

To all people who work to gain knowledge for the sake of our country, Palestine.

Shatha

Declaration

I certify that the thesis submitted for the degree of master is the result of my own research, except where otherwise acknowledged, and that this thesis (or any part of the same) has not be submitted for a higher degree to any other university or institution.

Signed: ……..

Shatha Al.Eman Sawalha

Date: 4.5.2018

Acknowledgements

I thank all who in one way or another contributed in the completion of this thesis. First and foremost I thank Allah for giving me the strength, knowledge, ability and opportunity to undertake this research study and to persevere and complete it satisfactorily.

I have great pleasure in acknowledging my gratitude to my supervisor Prof. Mieke Geens, Associate Professor at Research Group of Reproduction and Genetics (REGE) in Vrije Universiteit Brussels (VUB), for accepting me in her lab, teaching how to run the experiments, how to analyze results, and for being very collaborative after I returned home. You are a humble great teacher who has inspired me in stem cells field.

I also take pride in acknowledging my supervisor Prof. Zaidoun Salah, Associate Professor at Biology Department, Al Quds-Bard College for Arts and Sciences, in Al Quds University, in whom I have found a teacher, a role model and a pillar of support, his door has been always open for all students even if he is busy.

I would like to thank Stem Cell Lab at REGE, VUB with all its members, for having me over the last semester, and my colleagues in the lab for their kind efforts and support during my lab work. Thanks is conducted to Erasmus plus scholarship for letting this chance come true.

My acknowledgement would be incomplete without thanking the biggest source of my strength, my family, my mother, my father, my sisters and brothers. This would not have been possible without their unwavering love and support given to me at all times.

Sincere thanks to all my friends for their kindness and moral engorgement during my study.

Shatha Al.Eman Sawalha

May, 2018

Abstract:

During mammalian development, females inactivate randomly one of the two X chromosomes in a process called X-chromosome inactivation (XCI). This epigenetic event compensates the potential dosage differences of X-linked genes between sexes. The use of human pluripotent stem cells (hPSC) in regenerative applications and *in-vitro* modeling requires understanding of the XCI state and its impact upon generation of pluripotent cells. In this study, we investigated whether the XCI state of somatic cells had an influence on induced pluripoten stem cells (iPSC) reprogramming, through derivation of iPSC lines. We have generated ten iPSC from fibroblast of two healthy female donors (fibro "S", fibro "K") by lentiviral transduction of Yamanaka factors (OCT4, SOX2, KLF4 and c-MYC). The pluripotency state of the obtained iPSC lines was examined by immunoflurocence staining of protein surface markers: TRA-1-60, TRA-1-81,SSEA3, and SSEA4, and RT-PCR analysis for pluripotency-associated genes expression:*DNMT3B, GABRB3, GDF3, TDGF1 NANOG, POU5F1,* and *LIN28*. Furthermore, we tested XCI patterns of iPSC lines and their fibroblast donors through DNA methylation analysis. This analysis was performed for theandrogen receptor *(AR)* gene using the methylation restriction enzyme *HapII* (HUMARA assay).Also, XCI patterns were analyzed for seven iPSC lines that were used in a different project and were previously derived from the same donor (fibro "S").

The ten iPSC lines (S1,S2,S3,S4,S5,S6 from fibro S, and K1,K2,K3,K4 from fibro K) showed positive results for pluripotency characterization, and expressed most of pluripotency genes and surface protein markers.

The XCI results suggest that our iPSC lines were clonally derived from single fibroblast cells, since we observed non-random XCI pattern in all the lines that were derived. The fact that 5

out 6 S-lines and 4 out of 4 K-lines display skewing towards the same chromosome suggests that a particular X chromosome may confer a distinct advantage to these cells during cellular reprogramming or even during culture. Whether or not X chromosome reactivation occurs during reprogramming of these iPSC, it seems that the same X chromosome that was inactive in the paternal somatic cells is inactivated in the iPSC. However, the other seven iPSC lines which were derived earlier in the lab showed random XCI. This is in contrast with the results obtained in the newly derived iPSC lines and raises questions. It is possible that reactivation happened during reprogramming followed by random inactivation, or these cells were not clonally derived.

In conclusion, these results show a possible impact of XCI state upon iPSC reprogramming. To test this hypothesis, more experiments are needed with these iPSC lines and other lines derived from different donors.

Keywords: XCI, Skewed XCI, human pluripotent stem cells, induced pluripotent stem cells, culture advantage, DNA methylation analysis, HUMARA assay.

TABLE OF CONTENTS

LIST OF TABLES

LIST OF FIGURES

LIST OF ABBREVIATIONS

hPSC	Humann pluripotent stem cells
iPSC	Induced pluripotent stem cells
hESC	Human embryonic stem cells
XCI	X-chromosome inactivation
XIST	X inactive specific transcript
XIC	X inactivation center
PcG	Polycomb group
PGD	Preimplantation genetic diagnosis
SSEA3& SSEA4	Stage specific embryonic antigen 3 & 4
TRA-1-81 & TRA-1-60	Tumor resistance antigen 81 & 60
MEF	Mouse embryonic fibroblasts
LIF	Leukemia inhibitory factor
DMEM	Dulbecco's Modified Eagle's Medium
NS	Nutristem
PBS	Phosphate Buffered Saline
PFA	Paraformaldehyde
BSA	Bovin serum albumin
DMSO	Dimethyl sulfoxide
Pen/Strep	penicillin/Streptomycin
PCR	Polymerase chain reaction
RT-PCR	Real time –PCR
Ct	Cycle threshold
HUMARA	Human Androgen receptor assay
AR	Androgen receptor
DAPI	4',6-diamidino-2-phenylindole
DNA	Deoxyribonucleic acid
cDNA	Complementary DNA
RNA	Ribonucleic acid
OCT4 or POU5F1	Octamer-binding transcription factor 4

KLF 4	Krüppel-like factor 4
SOX2	SRY (sex determining region Y)-box 2
dNTPs	Deoxynucleotide triphosphate
RT	Room temperature
Bp	Base pair
µl	Micoliter
Ng	Nanogram
Pmol	Picomole
Mmol	Milimole

Chapter One

Introduction

1.1 X-Chromosome Inactivation:

In mammals, sex is determined by pair of sex chromosomes (X and Y), with males it being (XY) and in females (XX). This induces an imbalance between the X-linked genes between the sexes. In order to compensate this dosage differences, X-Chromosome Inactivation (XCI) has occurred in females. XCI is an epigenetic process by which most of the genes on one of the X-chromosomes in female cells are silenced and usually occurs during the late blastocyst stage of the embryo (Lyon, 1961). XCI results in a single transcriptionally active X chromosome in female cells, thus comparable to male cells. Selection of which X chromosome becomes inactivated is entirely random, that half of the cells inactivate the maternally inherited X chromosome and the other half the paternal X. However, once the choice has been made in a particular cell, it is stably propagated to all of its daughter cells.

1.2 Mechanism of XCI :

The process of XCI involves four steps that are regulated in a developmental manner: counting the number of X chromosomes, choosing which X chromosome to be inactivated, initiation of silencing the selected chromosome, and maintenance of stable repression of the inactive X (Xi) (Disteche & Berletch, 2015). Initiation is established by the long non-coding RNA X inactive specific transcript (*XIST),* which is transcribed from the chromosome that will be inactivated. *XIST* coats the areas where it is actively transcribed along this chromosome, and

forms a “cloud” by binding these areas. The covered areas lose RNA polymerase II, initiation factors, and other components that are necessary for transcription. However, there are regions on the inactivated X chromosome that sustain active transcription, also called “escape” inactivation, by looping out of the chromosomal territory covered by *XIST* (Briggs & Pera, 2014). Apart from XCI maintenance, all of XCI steps are orchestrated by the X-inactivation center (XIC).As the transition from initiation to maintenance occurs, the inactivation status become irreversible (Wutz, 2011). The maintenance phase involves a number of epigenetic processes such as alteration of DNA methylation and histone modification for Xi .The DNA methylation of CpG islands performed by the methylases DNMT3A/B and maintained by DNMT1. One example of histone modification is the accumulation of histone 3 lysine 27 trimethylation (H3K27me3) that silences transcription by the aid of Polycomb group (PcG) complex, which is a protein complex containing Ezh2 (enhancer of zeste homolog 2) and Eed (polycomb protein Eed). This complex is attracted by *XIST* accumulation on the Xi. The repression occurs when Ezh2 converts H3K27me2 (histone H3 lysine 27 dimethylation) to H3K27me3 (histone H3 lysine 27 trimethylation), a repressive histone mark. Another examples of histone modifications, is the loss of the active histone marks like histone H3 lysine 4 methylation (H3K4me) and H3 lysine 9 acetylation (H3K9ac), and thereplacement of histone H2A by macrohistone H2A (figure 1.1). All of these Xi characterizations lead to a strong condensation of the chromatin into a perinuclear structure, also known as the Barr body, ensuring long-term transcriptional silencing (Disteche & Berletch, 2015) (M Geens et al., 2016).

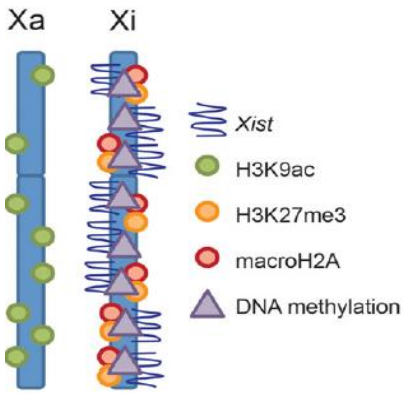

Figure 1.1 :Main molecular characteristics distinguish between active X chromosome (Xa) and inactive X chromosome (Xi) . (Mieke Geens & Chuva De Sousa Lopes, 2017)

1.3 Skewing of X-Chromosome inactivation :

Although the choice of which of the two X chromosomes is inactivated is entirely random, not all women have a 50:50 ratio of cells with one or the other X chromosome active. This case of non-random inactivation is called "skewing". Skewing of X chromosome inactivation is defined as a deviation of ≥25% from the balanced (50:50) inactivation of each parental X chromosome, in at least 75% of the female cells (Pomp et al., 2011). It has been shown to occur in X-linked diseases, but also in 10% of healthy females, mainly in tissues with high proliferation, such as the hematopoietic cells. There are different mechanisms that may lead to a non-random X-chromosome state such as: genetics factors or mutations, aging ,chromosomal rearrangements, and stochastic effects (Van den Veyver, 2001). Skewed XCI has also been linked to several pathologies such as intellectual disability, autoimmune diseases, such as autoimmune thyroid diseases (AITD), rheumatoid arthritis, and scleroderma. Also, aberrant XCI has been well documented in cancer but most data are only correlational (Mieke Geens & Chuva De Sousa Lopes, 2017). Consequently, determining the XCI states can be used as an indication of the presence of the diseases.

1.4 Stem cell potency :

Stem cells are undifferentiated cells found in embryos and adults, they have the ability to give rise to differentiated cells which are the building blocks of tissues and organs (Kolios & Moodley, 2013). Depending on the differentiation potency, stem cells are classified into different categories: totipotent, pluripotent, multipotent, and oligopotent stem cells (Figure1.2). Totipotent cells are the most undifferentiated cells found in early development that can produce all the differentiated cells in an organism. A zygote formed at egg fertilization and the cells that result from the first two divisions are totipotent cells, as they differentiate into both embryonic and extraembryonic tissues, forming the embryo and placenta (Mitalipov & Wolf, 2009).

Pluripotent stem cells defined as cells have the potential to differentiate into any cell types that arise from the three germ layers: ectoderm, endoderm, and mesoderm. Embryonic stem cells (ESC) are pluripotent cells were derived from inner cell mass of the blastocyst. Recently, pluripotent cells were generated by reprogramming of somatic cells, which defined as the reversal of the differentiation state of a mature cell to one that is characteristic of the undifferentiated embryonic state (Hochedlinger & Jaenisch, 2006). These generated cells called induced pluripotent stem cells (iPSC) had been derived by introducing four transcription factors (OCT4, SOX2, KLF4, and c-MYC) (Takahashi & Yamanaka, 2006).

Multipotent cells are derived from pluripotent cells and capable of differentiating into some cell types derived from a single germ layer, such as mesenchymal stem cells which can differentiate into mesoderm-derived tissue such as adipose tissue, bone, cartilage, and muscle (Kolios & Moodley, 2013). Oligopotent or unipotent cells are able to form a few lineages, in oligopotent cells, or only one lineage (unipotent cells) within a specific tissue. Hematopoietic

stem cells are an example of oligopotent cells, they can differentiate into both myeloid and lymphoid lineages (Marone et al., 2002).

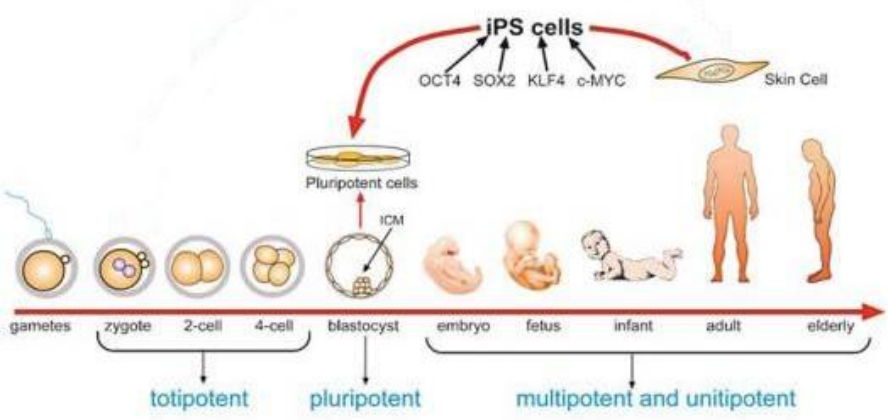

Figure 1.2: Classification of stem cells on the basis of potency into totipotent, pluripotent, multipotent , oligopotent and unipotent cells (Mitalipov & Wolf, 2009).

1.5 Human Pluripotent Stem Cells (hPSC) as disease cellular models:

Human pluripotent stem cells (hPSC), which include human embryonic stem cells (hESC) and human induced pluripotent stem cells (hiPSC), can self-renew indefinitely in culture and had the ability to become almost any cell type in the human body. Therefore, hPSC is used for cell replacement therapy and cellular modeling for human diseases and development.

Understanding human development and the diseases caused by developmental and genetic defects, is one of the major challenges in biology. Much of our knowledge about human development has been extrapolated from studies of animal model organisms, since we cannot study human development in the same way we do when experimenting on a mouse or fruit fly. These models have produced key insights into the general principles of human development, disease mechanisms, as well as into the genes and signaling pathways that control specific aspects of cell fate specification and tissue morphogenesis (Zhu & Huangfu, 2013). Despite

these benefits, there are notable limitations of using animal models. First, animal models do not accurately mimic the disease in human cells, as a result of species-specific differences between the animal system and that in humans. Another limitation rises from the genomic variation of the human and murine models; since around 1% of human genes have no identifiable mouse homologs (Consortium, 2001). Also, many genetic variants associated with human disease fall in the non-coding regions that show relatively little conservation, raising the possibility to get different phenotypes of human disease if we used animal variants. Furthermore, the majority of drugs that are effective in mice have failed in human clinical trials. Moreover, generating and breeding transgenic animals is expensive and time consuming (Merkle & Eggan, 2013).

Using hPSC is an essential complement with animal models to overcome these limitations. The potential of hPSC to differentiate to each cell type and its self-renewal capacity with rapid, cost-effective *in-vitro* culture offers an attractive window to understand human normal and abnormal development or pathogenesis of human diseases. Modeling human diseases ‘‘in a dish” started with hESC ; Thomson and colleagues derived hESC lines by culturing human blastocysts in a cocktail of growth factors and supporting mouse feeder cells (Thomson et al., 1998). By Performing preimplantation genetic diagnosis (PGD) on embryos, one of the methods that used to predefine gene mutations, researcher were able to derive ‘‘disease-specific’’ hESC from the identified genetic disorders such as for cystic fibrosis, Huntington’s disease, and Fragile X syndrome. However, PGD embryos are available only for a limited number of human diseases. The forward genetic approach have also been utilized with hESC, by generating mutation in genomic loci with a specific disease at hESC, followed by the identification of a disease phenotype in hESC or their derivatives. This approach is limited to

the inefficient methods to genetically modify hESC. Neither all diseases are genetically known nor disease phenotype could be screened in hESC (Saha & Jaenisch, 2009).

In a more recent breakthrough, reprogramming of mouse adult cells through viral transduction of four transcription factors (OCT4, SOX2, KLF4, and c-MYC) to produce induced pluripotent stem cells (iPSC) was reported by Yamanaka and colleagues in 2006. One year after, they generated human iPSC from human fibroblasts (Takahashi et al., 2007). Using this combination of Yamanka transcription factors is necessary and sufficient to return terminally differentiated cells to a pluripotent state. These iPSC are capable of generating tissues of all three germ layers, similar to the capacity of human embryonic stem cells (hESC). This techniques has also been applied to blood or skin samples harvested from patients diagnosed with specific diseases; allowing researchers to study the roles of a specific gene in developmental cell fate decisions and the physiological functions of disease-relevant cells (Saha & Jaenisch, 2009).

Generation of "Disease-specific" hiPSC lines from patients with many types of diseases could provide immune-matched supply of pluripotent cells, that can be used in multipurpose research and clinical applications. "Disease-specific" iPSC have been generated for various diseases; hematopoietic, hepatic ,endothelial, neurological, and cardiovascular diseases and the number is increasing, reflecting their growing utility as models for studying disease development, as well as platforms of drug screening and toxicity testing to investigate therapeutic agents (Ebert, Liang, & Wu, 2012). Furthermore, this approach of iPSC can be used to generate therapeutic cells for replacement therapy that may avoid immune rejection in the transplant recipient, since it can be generated directly from the patient.

1.6 Characterization of iPSC :

As iPSC are very similar to hESC, the criteria used to characterize iPSC are very close to which employed to ESC research. Initially, the morphology of iPSC under microscope, is the first character used to identify potential iPSC. iPSC form-colonies of compact cells exhibiting a high nucleus to cytoplasmic ratio with a round tight shape and smooth borders. Moreover, iPSC and ESC have comparable growth rate, elevated telomerase and alkaline phosphatase activities. In addition, iPSC express specific cell surface proteins such as stage-specific embryonic antigen (SSEA)-3, SSEA-4, TRA-1-60, TRA-1-81, and pluripotency markers as:*NANOG, OCT3/4, TDGF1, DNMT3B, GDF3, GABRB3,* and *LIN28*. Gene expression of pluripotency markers is very essential to identify the plurioptent state of cells, since the clonality of iPS maybe different among the cells even if they are generated under identical conditions. This might because the cells are at different stages of reprogramming, or incomplete reprogramming that may render them to differintation with increased potential to teratomas formation (Ng & Choo, 2010). Masaki and colleagues observed that even alkaline phosphatase (ALP)- positive colonies can be categorized into 40 groups based on the gene expression pattern of 8 marker genes: *NANOG, TDGF1, DNMT3B, ZFP42, FOXD3, GDF3, CYP26A1* and *TERT,* indicating the importance of characterization of endogenous pluripotency gene markers (Masaki et al., 2008). In table 1.1 we summarize the markers that we used in our work.

As there is a difference between iPS and ES cells according to the reprogramming in iPSC, monitoring karyotype stability during culture is also needed for extended culture of both iPSC and human ES cells. Moreover, methylation status and differentiation into somatic cell types in vitro and in vivo are useful for testing stem cell pluripotency.

Table 1.1 List of genes and antigen markers used for iPSC pluripotency characterization in our work, and their role of function from literature and NCBI website.

Marker	**Type**	**Role of function**
NANOG	Gene/ antigen	Establishment of pluripotency, resisting differentiation
OCT 3/4	Gene/ antigen	Essential for generation iPSC , maintain pluripotency
SSEA 3/4	Antigen	Stage-specific embryonic antigen, cell surface glycolipid
TRA-1-60	Antigen	Stem cell surface keratan sulfate antigen epitope
TRA-1-81	Antigen	Stem cell surface keratan sulfate antigen epitope
LIN28	Gene	Regulator of genes involved in developmental timing and self-renewal in embryonic stem cells
DNMT3B	Gene	DNA methyltransferase 3 beta, play role in DNA methylation that is important for human development, imprinting, X chromosome inactivation
GDF3	Gene	Growth differentiation factor 3, encodes protein plays a role ocular and skeletal development.
GABRB3	Gene	Gamma-aminobutyric acid type A receptor beta3 subunit, encodes a member of the ligand-gated ionic channel family.
TDGF1	Gene	Teratocarcinoma-derived growth factor 1, encoded proteins that play an essential role in embryonic development and tumor growth.

1.7 XCI in hPSC and hiPSC :

Human pluripotent stem cells are classified into three classes according to their X chromosome state (Figure 1.3). Class I cells contain two active X chromosomes (XaXa) in the undifferentiated state and are considered closest to ground state pluripotency. Upon placing class I cells under differentiation conditions, *XIST* transcription initiates from the prospective Xi and random XCI begins. Class II cells have already initiated XCI (XaXi) and express *XIST* RNA even in the undifferentiated state. Finally, class III cells still retain XCI but have lost *XIST* expression, show accumulation of repressive histone modifications and often also XCI-specific DNA methylation. This occurs regardless of whether they are growing in undifferentiated or differentiated conditions (Lessing & Lee, 2013). Class I is rare in humans, class II, III are more likely to happen.

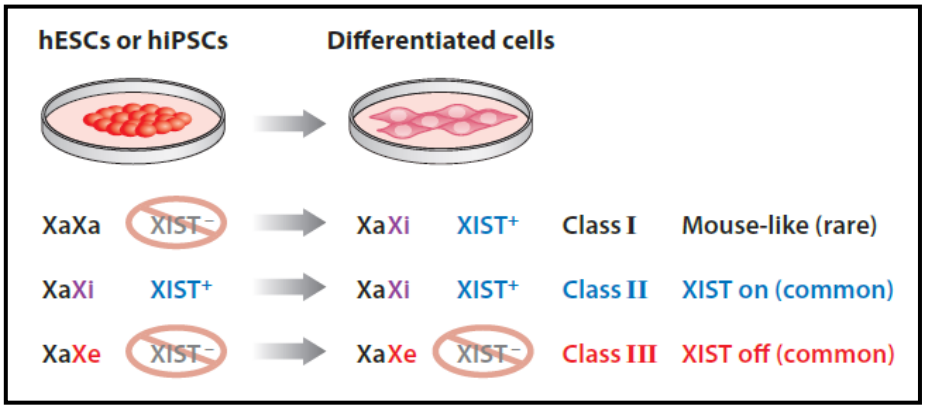

Figure 1.3: Classification of human pluripotent stem cells (hPSC) according to XCI state (Lessing & Lee, 2013)

Studying the XCI state in hPSC has gained enormous interest and importance in disease modeling, as XCI markers have provided one of the few readouts of the pluripotent state.

Upon the discovery of iPSC, a new subfield of characterization of XCI emerged. In mouse iPSC, it has been shown that reactivation happens during reprogramming. However, the X chromosome states during reprogramming of human iPSC is contradictory and complex. Some

groups such as Marchetto et al., reported reactivation of the X chromosome (XaXa) in iPSC colonies made from female Rette syndrome patients (Marchetto et al., 2010). On the other hand, Tchieu et al.showed that the X chromosome remains inactive (XaXi) and X chromosome reactivation never happens (Tchieu et al., 2010). They also obtained clonal hiPSC population exhibiting XCI. It is worth noting here that Lessing et al have summarized XCI status of hiPSCs from multiple labs (Lessing & Lee, 2013).

There are reports regarding the variability in XCI of the same reprogrammed colony states. Bruck et al. reported that a single clone may contain cells of different states, Indicating that the variability is based on biological factors, not methodology. Also, they proposed a model of the dynamics of XCI in pluripotent stem cells (Bruck & Benvenisty, 2011). These differences raise questions about the stability of hiPSC cells and their impact on clinical trials, raising the need for careful characterization of their properties. In contrast, recent work of Tomoda and Yamanka et al. studied the effect of culture conditions and derivation on the epigenetic features of X chromosome in hiPSC. They used SNL feeders, which are immortalized mouse embryonic fibroblasts (MEF) that produce high levels of leukemia inhibitory factor (LIF), to derive and maintain hiPSC. They reported that the Xi of donor fibroblast was frequently reactivated (Xa/Xa) upon early passage on SNL, compared to non-frequent production of Xa/Xa when non-SNL feeders were used. Therefore, choosing the desired pattern Xa/Xi or Xa/Xa for the derived hiPSC is possible and could be useful in disease modeling and clinical applications (Tomoda et al., 2012).

In order to determine whether a preferential XCI exists in hPSCs and whether the XCI pattern changes during long-term culture or upon differentiation, Geens et al., investigated the XCI

state in different female hPSC lines: two hiPSC and 21 hESC lines. The results shows that hPSC rapidly lose XCI marks during culture and become *XIST*-independent XCI state with loss of repressive histone modifications and often erosion of methylation. Also, they reported high incidence of non-random XCI related methylation pattern. This skewing of XCI pattern is independent from the origin of the X chromosome from paternal or maternal and is not occurring as passenger event, as chromosome aberration lead to culture take over. Most probably, XCI skewing driven by specific X-linked allele, that is activated or repressed, confers growth advantage to the cells (M Geens et al., 2016).It is also worth noting Pomp et al. study that proposed the cause of XCI skewing in hiPSC. They found that all iPSC colonies, which were derived from the same fibroblasts, contain the same inactive X. This skewed choice may be due to more efficient reprogramming of the donor fibroblast in which the dominant X was active. Notably,the skewing can be alleviated by introducing telomerase activity to these cell cultures (Pomp, Dreesen et al., 2011).

XCI skewing in hiPSC have implications for using of female hiPSCs in clinical applications and disease modeling, especially for X-linked disease. Investigate the XCI state in hiPSC and whether it is compatible with the desired application, is an essential step before using it.

1.8 Aim Of The Study:

From the literature, it seems that the XCI status may have a direct impact on the potential to generate hPSC and on their pluripotent status in vitro. The fact that most several labs report a very fast skewing of XCI patterns suggests that the presence and activity of specific X-linked alleles may directly confer a culture advantage (or disadvantage) to the cells. We would like to further investigate whether this can be true. A nice set-up would be to perform competition experiments with sublines of the same hESC line, but displaying an opposite skewed XCI pattern. However, all the hESC lines available in our lab already displayed a completely skewed XCI pattern, which did not allow us to derive clonal sublines with opposite XCI patterns. Therefore, we have worked on generating iPSC from fibroblast of healthy human females, to investigate if X chromosome inactivation status influences the efficiency of hiPSC reprogramming by studying XCI methylation related patterns in the derived iPSC lines.

1.9 Objectives :

1. To generate iPSC from two healthy female fibroblast by lentiviral transduction of Yamanaka factors (OCT4, SOX2, KLF4 and c-MYC).
2. To characterize the pluripotency state in the derived iPSC lines by performing immunoflurocence staining for surface protein markers (TRA-1-81, TRA-1-60, SSEA3 and SSEA4) and gene expression by RT-PCR for pluripotency marker genes (*DNMT3B, GABRB3, GDF3, TDGF1, LIN28, NANOG,* and *OCT4*).
3. To investigate the XCI state of the derived iPSC by studying the methylation state of the X-chromosome using HUMARA assay.

1.10 Significance of The Study:

Studying the XCI state in female hPSC is one of the major epigenetic factors that should be examined before any clinical applications. According to observing early skewing XCI in female hPSC, this study emphasizes the possibility of the presence of an X-linked event that gives cells with a specific XCI pattern a culture advantage over other cells and recommends further research to prove this hypothesis.

Chapter Two

Materials and Methods

2.1 Generation of human induced pluripotent stem cells (hiPSC):

Two fibroblast lines (fibro "S", fibro"K") from human healthy females were used for human iPSC derivation using lentiviral transduction with thpRRL.PPT.SF.hOKSM.idTomato.preFRT vector which contains the four Yamanaka factors: C-MYC, KLF4, SOX2 and POU5F1. Fibroblasts, which were derived from skin biopsies, were thawed and grown in mouse embryonic fibroblast (MEF) medium consisting of DMEM (Thermo Fisher Scientific), supplemented with 20% heat inactivated fetal bovine serum (Thermo Fisher Scientific), 2 mM L-glutamine (Thermo Fisher Scientific) and 100 U/ml Pen/Strep (Thermo Fisher Scientific). One day before transduction, fibroblasts were plated in a 6-well plate at a density of 2.5×10^4 cells/cm^2. The transduction mix which consists of 1×10^5 virus particles per well and protamine sulfate (10 µg/ml final concentration) was prepared and incubated for 15 minutes at room temperature (RT). Two ml of the mix was added per well and the cells were incubated at 37^oC, 5% CO_2 for 24 hours. In the following days, the cells were washed three times with warm PBS and MEF medium was changed daily. Cells were passaged to coated dishes with Laminin (LN521) in Nutristem (NS) medium one week after plating. Single iPSC colonies were isolated based on ESC-like morphology. Six colonies from "S" fibro line and 4 colonies from "K" fibro line were mechanically isolated and further cultured on LN521-coated 24-well plates in NS medium, afterwards each isolated colony grew into an iPS cell line. Once the

cultures were confluent, they were passaged using TrpLE^{TM} Express (Thermo Fisher Scientific) in ratios ranging from 1:10 to 1:50.

2.2 Immunofluorescence Staining:

2.2.1 Fixation:

Cultured iPSC lines on LN521 coated 4-well plates, were first washed twice with PBS for five minutes to each. Fixation was performed with 3.7% paraformaldehyde (PFA) (Sigma-aldrich) in PBS for 15 minutes at RT. After that, the plates were washed again as above. The fixed cells were stored in PBS at +4 °C.

2.2.2 Staining (immunofluorescence):

Before adding primary antibodies, cells were permeabilized with 0.1% Triton X-100 in PBS. Plates were incubated for 10 minutes, then washed three times 10 minutes with PBS. Blocking solution (3% of Bovin serum albumin (BSA) in PBS) was used to reduce non-specific antibody binding, therefore, 500µL of the solution was added to the wells and incubated for one hour at room temperature.

Four primary antibodies (TRA-1-60, TRA-1-81, SSEA, SSEA4) were used to detect surface antigens. For antigen-antibody binding detection, secondary antibodies with fluorescent dye were added specifically to each primary antibody. In table 2.1 & 2.2, are listed the names of the primary and secondary antibodies used, with their dilution ratio.

Table 2.1 List of primary antibodies:

Primary Antibodies (against human protein)	**Dilution ratio**	**Reference number & company**
TRA-1-81 mouse IgM	1:100	MAB 4381, Merck
SSEA3 rat IgM	1:50	MAB 4303, Merck
SSEA4 mouse IgG	1:100	MAB 4304, Merck
TRA-1-60 mouse IgM	1:100	MAB 4360, Merck

Table 2.2 List of secondary antibodies:

Secondary Antibodies	**Dilution ratio**	**Reference number & company**
Alexa 488 goat anti-mouse IgM	1:200	A21042, Thermo Fisher Scientific
Alexa 488 goat anti-rat IgM	1:200	A-21212, Thermo Fisher Scientific
Alexa 488 goat anti-mouse IgG	1:200	A11029, Thermo fisher Scientific

After preparing the diluted primary antibodies, 300µL of each specific antibody was added to each well of the cells. The plates were wrapped with parafilm and kept overnight at 4^{o}C.

The next day, the primary antibodies were removed and the wells were washed with PBS three times. Then, 300 µL of the diluted secondary antibodies were added to the wells, based on which primary antibody was there. The plates were covered with aluminum foil to avoid the light and incubated at room temperature for two hours. After removing the secondary antibodies, the wells were washed three times with PBS. 300 µL of Hoechst 33342 (H3570, Thermo fisher Scientific), a nuclear stain, were added to each well and incubated for 10 to 15 minutes in dark at room temperature. This stain was diluted 1:2000 with PBS before adding. After removal of Hoechst and washing with PBS, one drop of prolong Gold Anti-fade reagent (Thermo Fisher Scientific) was added to each well and covered with coverslip. The plates

were kept in the fridge at 4^{o}C, protected from the light. The stained cells were analyzed using the IX-81 fluorescent microscope (Olympus) with Cell^F software (Olympus).

2.3 Gene expression for pluripotency markers:

2.3.1 Pellet collection:

Cell pellets from hiPSC and fibroblast lines were needed for molecular analysis. As the cells appeared confluent under the microscope, it was ready for passage and pellet collection. First, the cells were incubated with TrypLE^{TM} (Thermo Fisher Scientific) for 5 minutes, then diluted with PBS. The deattached cells were collected for centrifugation at 1000 rpm for 5 minutes. The supernatant, that appeared after centrifugation, was aspirated and the pellets resuspended in PBS for washing. Then, the cells were centrifuged again and the supernatant was discarded. The pellet tubes were stored at -80^{o}C.

2.3.2 RNA extraction with spin column method:

RNA extraction from cell pellets was carried out using RNeasy Mini Kit, (QIAGEN) using the manufacturer's protocol. In brief, the cells were disrupted by adding lysis buffer RLT, that the volume of the buffer is selected according to number of pelleted cells. The lysate was passed through needle syringe to be homogenized, then an equal volume of 70% ethanol was added to the homogenized lysate. The sample was transferred to a spin column and centrifuged at 10,000 rpm for 30 seconds. After a first washing step with 700 µl washing buffer RW1, DNase treatment was performed. The DNase mix, which consists of 10 µl DNase stock solution with 70µl RDD buffer, was directly added to the column membrane and incubated for 15 minutes at benchtop. After that, the sample was washed again in 350 µl RW1 twice.

Finally, RNase-free water was added directly to the spin column membrane and RNA was eluted by spinning. The obtained RNA was stored at -80^{o}C.

2.3.3 Complementary DNA (cDNA) transcription:

First-strand cDNA synthesis was performed using First-Strand cDNA Synthesis Kit, (GE Healthcare). 8µl of RNA solution was incubated at 65^{o}C for 10 minutes. The reaction mix, which consists of 5µl bulk first-strand cDNA reaction mix, 1 µl primer, 1µl DTT solution, was prepared for each sample. Then, the mix was added to the RNA solution and the tubes were incubated at 37^{o}C for 1 hour. The completed first-strand cDNA reaction product was ready and it was stored at 4^{o}C.

2.3.4 Gene expression by RT-PCR:

The ten derived iPSC lines were analyzed for gene expression of pluripotency markers (*DNMT3B, GABRB3, GDF3, LIN28, NANOG, POU5F1* and *TDGF1*) by qRT-PCR (Viia 7 thermocycler, ViiA 7 software version 1.2; Thermo Fisher Scientific). *GUSB* and *UBC* were used as housekeeping genes for the reactions. The two fibroblast cultures from which the hiPSC were derived, were used as negative control. Reactions were performed using TaqMan® Fast Advanced Master Mix (Thermo Fisher Scientific) with 5ng/µL of cDNA from the cells (8 µl of 1300 ng /cDNA input per well). Assays for *GABRB3, TDGF1, GDF3, DNMT3B* and *GUSB* were performed according to published protocols (Supplementary Table 1), whilst for all other genes, primers and probes were designed in-house (Supplementary Table 2). Amplification conditions were the following: 20 seconds at 95°C and 40 cycles of 1 second at 95°C and 20 seconds at 60°C.

2.4 HUMARA assay:

The human androgen receptor (HUMARA) assay, a polymerase chain reaction (PCR)-based X-chromosome inactivation assay, was used to investigate the X-chromosome inactivation pattern. This assay makes use of the difference in DNA methylation between active and inactive X-chromosome and the highly polymorphic GAC repeats in the androgen receptor (*AR*) gene.

The HUMARA assay was performed as follows:

2.4.1 DNA Extraction with spin column method:

DNA extraction from cell pellets was performed using the DNeasy® Blood & Tissue Kit, QIGEN. 20 µl of proteinase K and 200µl of lysis buffer were added and the samples were incubated at 56^{o}C for 10 minutes. Then 200µL of 100% ethanol was added. In order remove undesired components, the mixture was transferred into 2mL spin column placed in collection tube and centrifuged. Two washes with 500 µl of washing buffers AW1 and AW2, respectively, were performed. After the spin column was transferred to a microcentrifuge tube, 100 µl of eluting buffer (AE) was added and centrifuged. The obtained DNA from each sample was stored at 4^{o}C.

2.4.2 DNA digestion:

The extracted DNA from cells (hiPSC and fibroblast) was digested using the methylation sensitive restriction enzyme *HpaII* (Anza ^{TM} 93 HpaII, Thermo Fisher Scientific). This enzyme recognizes C^CGG sites and cuts unmethylated DNA. A mix with 20µl total volume was prepared containing 1µL *HapII*, 2µL buffer (Anza ^{TM} 10X buffer, Thermo Fisher Scientific)

and 100ng DNA. All samples were incubated at 37^{o}C for 4 hours, then 1 µl *HapII* enzyme was added. The samples were left overnight at 37^{o}C. In each experiment, DNA from a male sample was used as control for digestion, since the male X chromosome is unmethylated and these samples should thus be completely digested.

2.4.3 Detection of the XCI pattern:

To evaluate the level of inactivated X chromosomes, PCR for each DNA sample (digested and undigested) was performed to amplify the CAG repeat region in the first exon of the (*AR*) gene. The reaction mix, in total volume of 25 µl, consisted of: 10% 10X AmpliTaq PCR buffer II, 2 mM $MgCl_2$, 10 pmol of primers (TCCAGAATCTGTTCCAGAGCGTGC and GCTGTGAAGGTTGCTGTTCCTCAT), 0.2 mmol dNTP, 2.5% DMSO, 1.25 U of Amplitaq polymerase and 20 ng DNA.PCR conditions were as follows: 5 min at 95^{o}C, followed by 35 cycles of 30 sec at 95^{o}C, 30 sec at 58^{o}C, and 30 sec at 72^{o}C. Then, 7 min at 72^{o}C and the temperature decreased to 8^{o}C until the end. The PCR products were analyzed by gel electrophoresis and capillary electrophoresis ABI 3730 genetic analyzer (Applied Biosystems, Foster City, CA) using internal-lane size standard and Gene Mapper software (Applied Biosystems).

Chapter Three

Results

3.1 Female hiPSC lines express pluripotencey markers

3.1.1 iPSC morphology

In order to generate iPSC from human fibroblast, we introduced the lentiviruses containing Yamanaka factors into fibro "K" and fibro "S" (Figure 3.1-A,B). After two weeks of transduction, we observed small compact iPSC colonies, which resembled hES colonies (figure 3.2-A,B). The colonies showed clear exponential growth during the followingdays (Figure 3.2-C), they were flat with distinct borders in contrast to surrounding fibroblasts. Afterwards, we manually picked the colonies, to generate iPS cell line (figure 3.2- D,E,F).

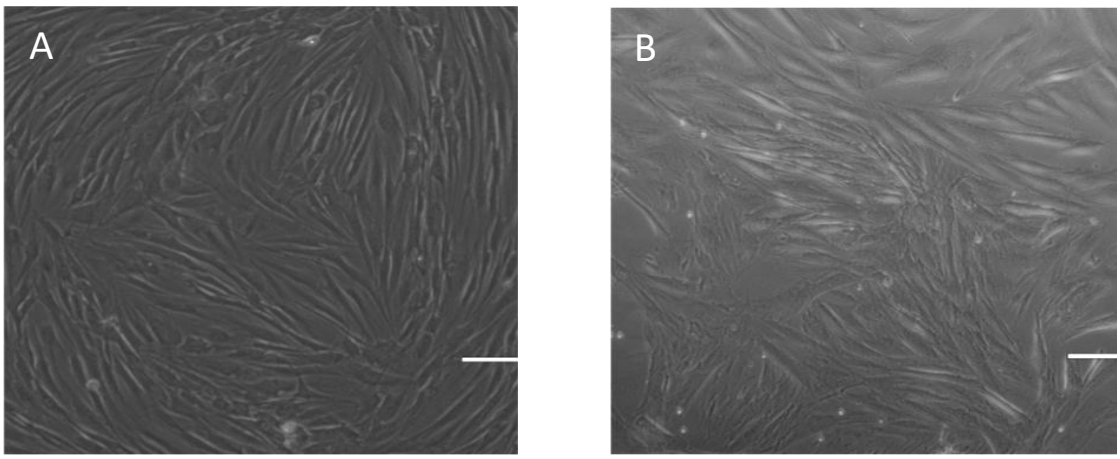

Figure 3.1: Microscopic images for fibroblasts obtained from two donors.A) Fibro "K" and **B)**Fibro "S" before transduction, scale bar: 1000 μm.

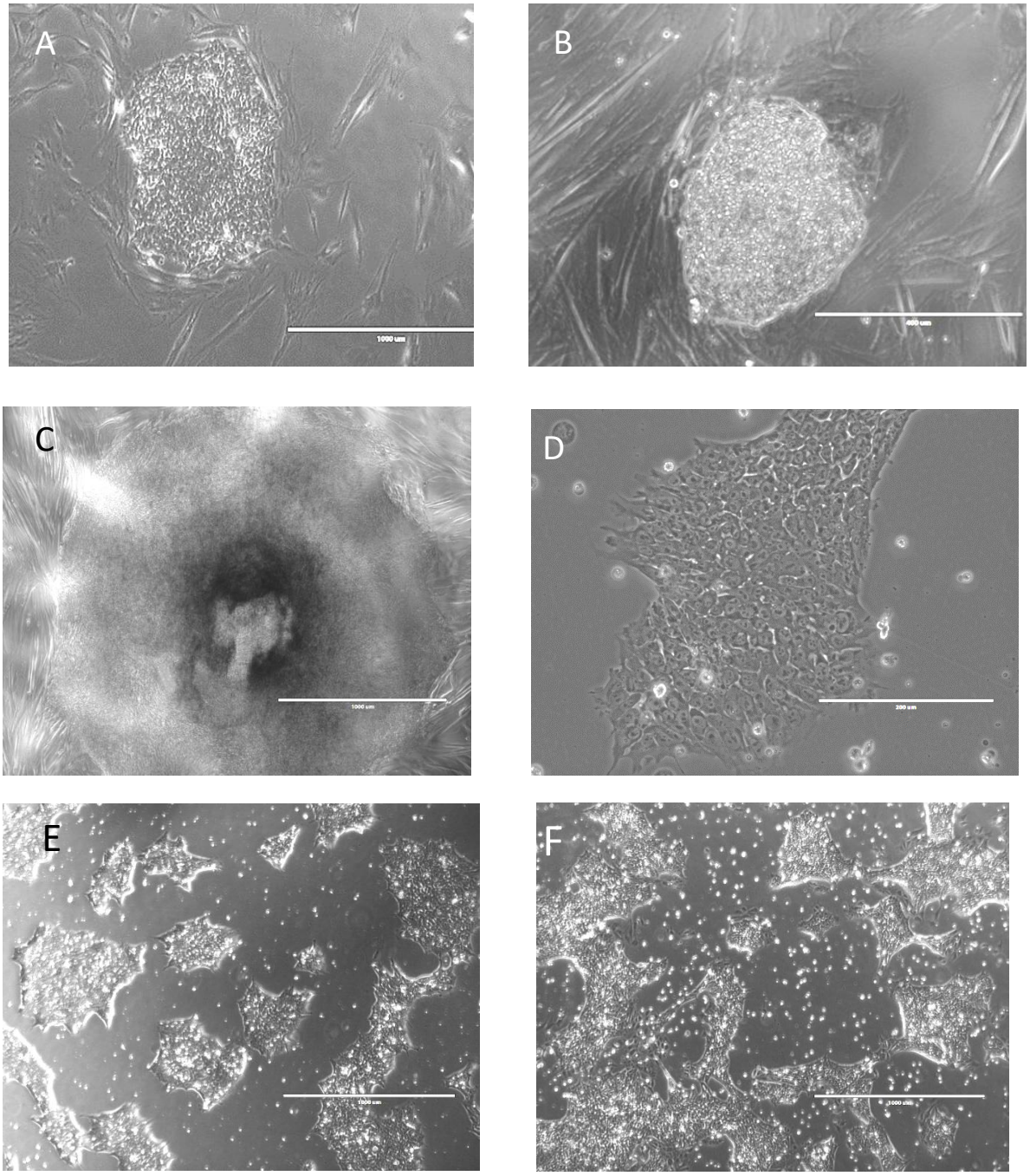

Figure 3.2: **Microscopic images for iPSC lines**.**A&B)** Micrographs of iPSC coloniesobtained "K" (A) and "S" (B) fibroblasts. Scale bar: 1000µm and 400µm , respectively.**C)** expanded iPSC colony after 20 days of transduction, scale bar: 1000µm. **D)** iPSC S1, one of iPSC line was generated after picking one of fibro "S" colonies, scale bar: 200µm. **E)** iPSC K4, one of iPSC line generated from fibro "K", scale bar: 1000µm. **F)** iPSC S4, one of iPSC line generated from fibro "S", scale bar: 1000µm.

3.1.2 Expression of surface protein markers as assessed by immunoflurosence staining

Since the expression of hES cell-specific surface antigens (TRA-1-60, TRA-1-81, SSEA3,SSEA4) is an indicator of the pluripotencey state, we performed immunoflurosence staining for the derived iPSC lines. All the ten iPSC lines showed positive staining for the pluripotency markers tested, except iPSC S3, compared to fibroblast control (Figure 3.3). These results indicate that we were able to successfully generate iPSC lines from the transformed fibroblasts. Supplementary Figure 1 displayed the fluorescence microscope images for the rest of iPSC lines; iPSC S4,S5,S6 derived from fibro “S”, and iPSC K3, K4 derived from fibro “K”.

Figure 3.3-A:

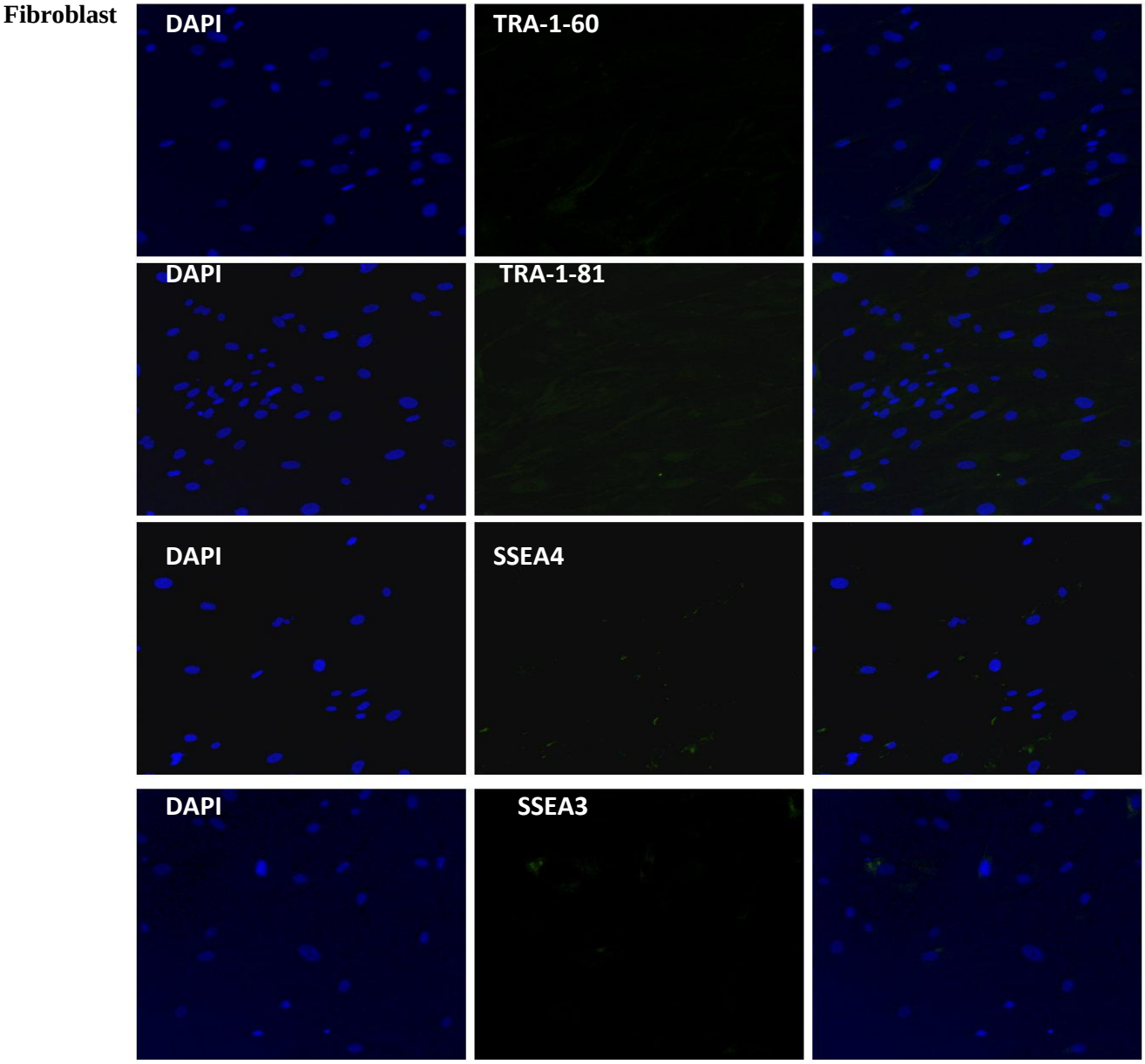

Figure 3.3-A: Expression of surface protein markers of fibroblast by immunoflurosence staining. Fluorescence microscope images for fibroblast after staining them for surface markers TRA-1-60, TRA-1-81,SSEA3, and SSEA4. Blue color of DAPI represent nuclear counter stain. Green color represents the specific staining of the intended markers. The stained cells were analyzed using the IX-81 fluorescent microscope (Olympus) with Cell^F software (Olympus).

Figure 3.3-B:

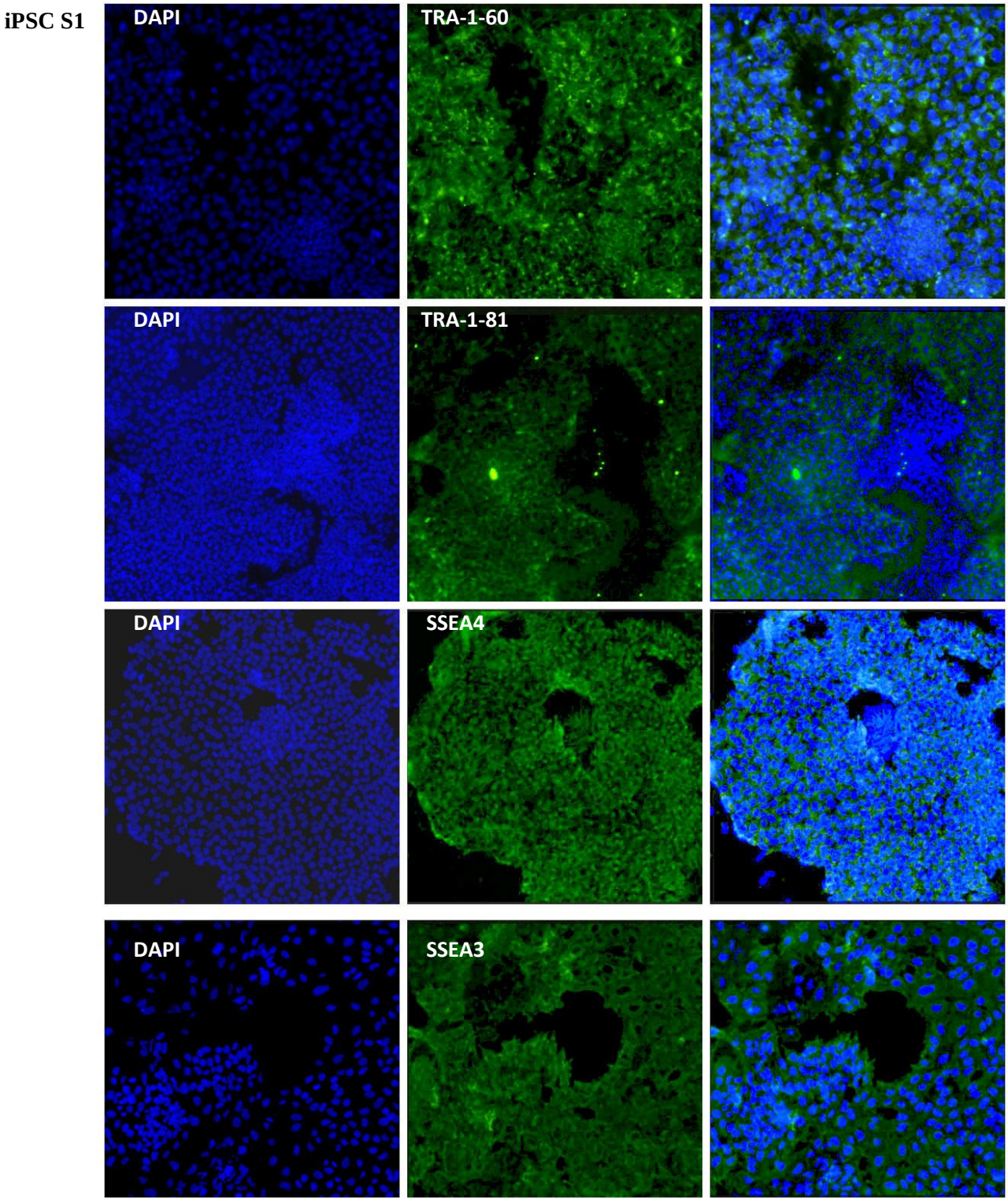

Figure 3.3-B: Expression of surface protein markers of iPSC S1 by immunoflurosence staining. Fluorescence microscope images for iPSC S1 after staining them for surface markers TRA-1-60, TRA-1-81,SSEA3, and SSEA4. Blue color of DAPI represent nuclear counter stain. Green color represents the specific staining of the intended markers. The stained cells were analyzed using the IX-81 fluorescent microscope (Olympus) with Cell^F software (Olympus).

Figure 3.3-C :

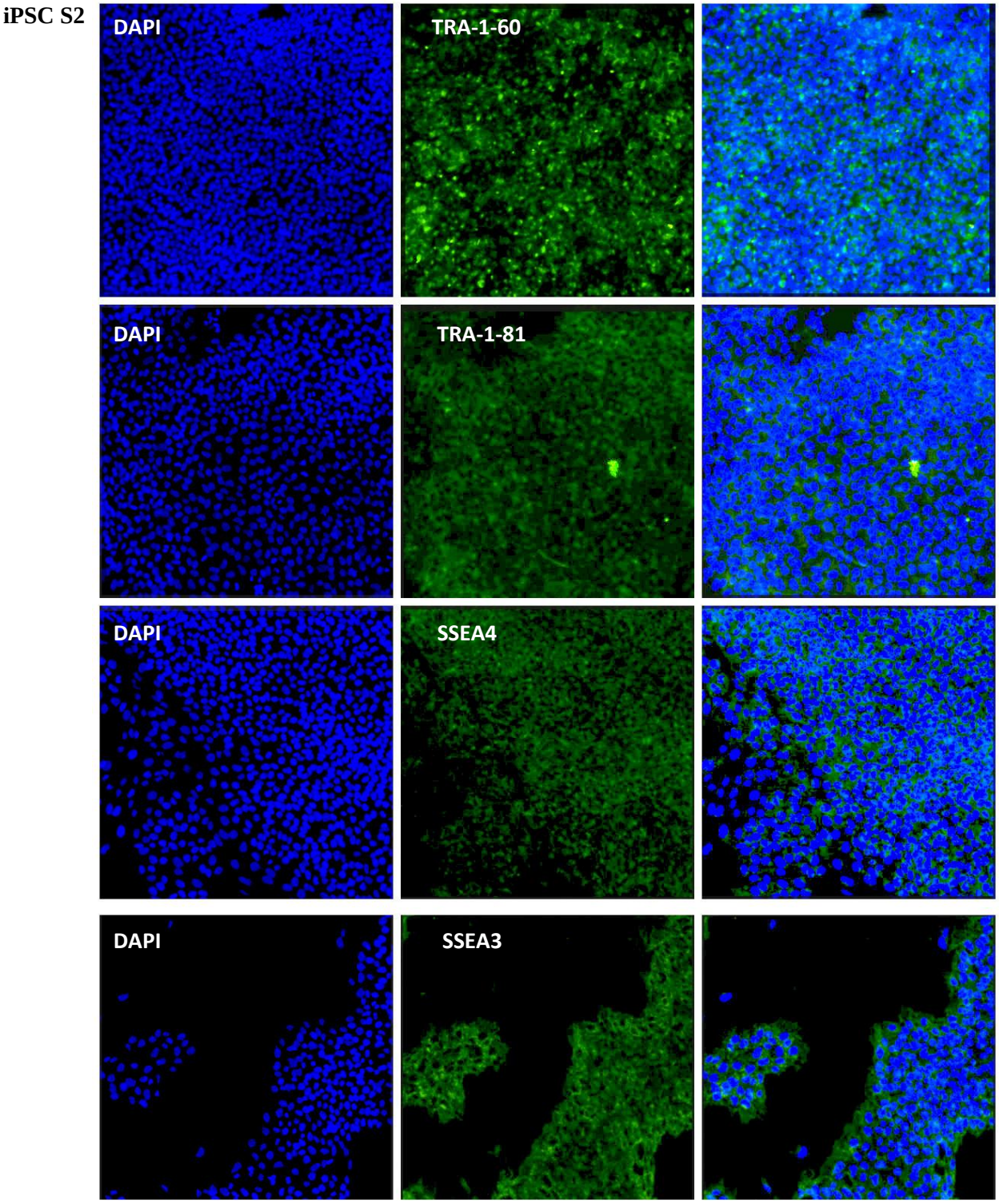

Figure 3.3-C: Expression of surface protein markers of iPSC S2 by immunoflurosence staining. Fluorescence microscope images for iPSC S2 after staining them for surface markers TRA-1-60, TRA-1-81,SSEA3, and SSEA4. Blue color of DAPI represent nuclear counter stain. Green color represents the specific staining of the intended markers. The stained cells were analyzed using the IX-81 fluorescent microscope (Olympus) with Cell^F software (Olympus).

Figure 3.3-D :

iPSC K1

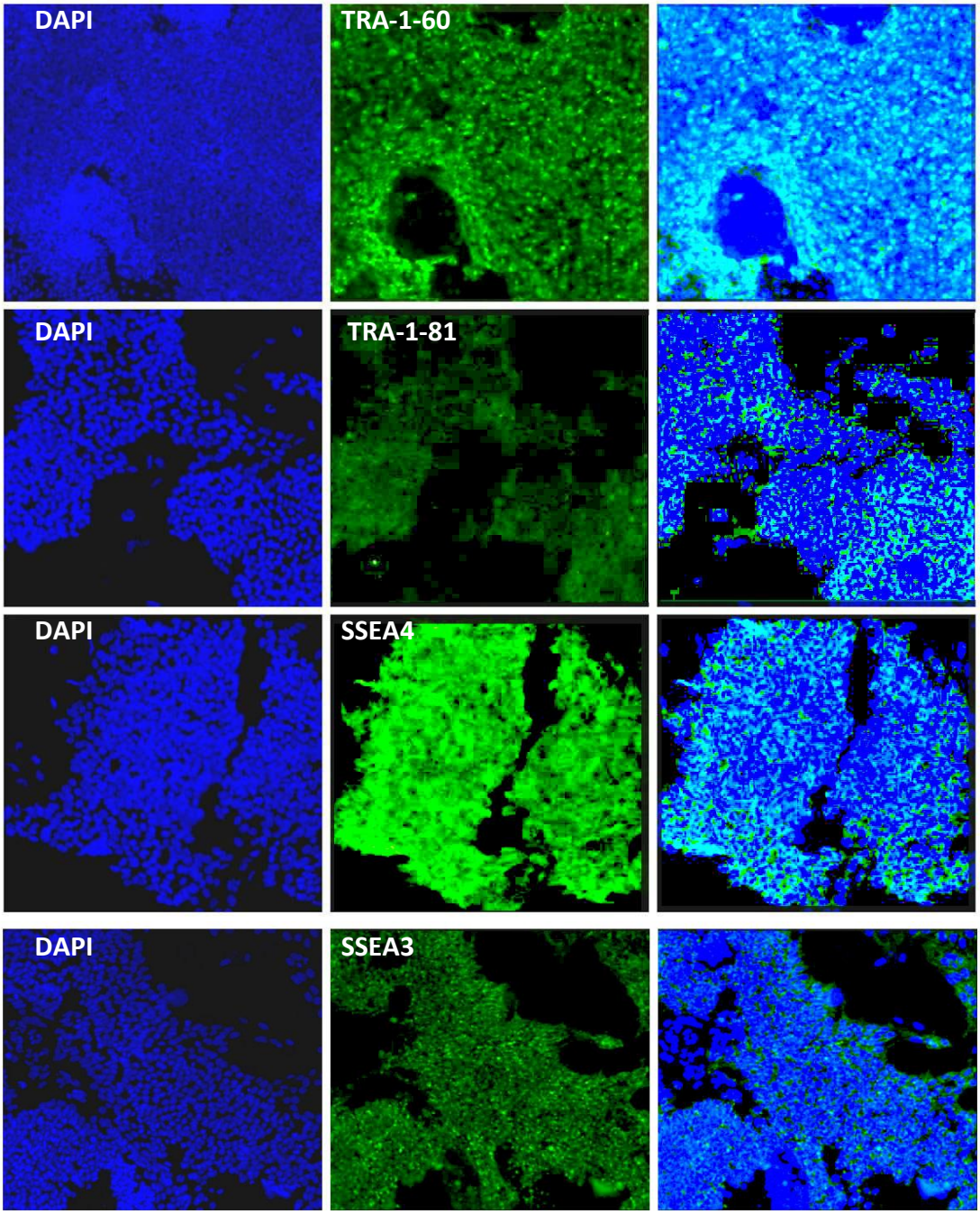

Figure 3.3-D: Expression of surface protein markers of iPSC K1 by immunoflurosence staining. Fluorescence microscope images for iPSC K1 after staining them for surface markers TRA-1-60, TRA-1-81,SSEA3, and SSEA4. Blue color of DAPI represent nuclear counter stain. Green color represents the specific staining of the intended markers. The stained cells were analyzed using the IX-81 fluorescent microscope (Olympus) with Cell^F software (Olympus).

Figure 3.3-E:

iPSC K2

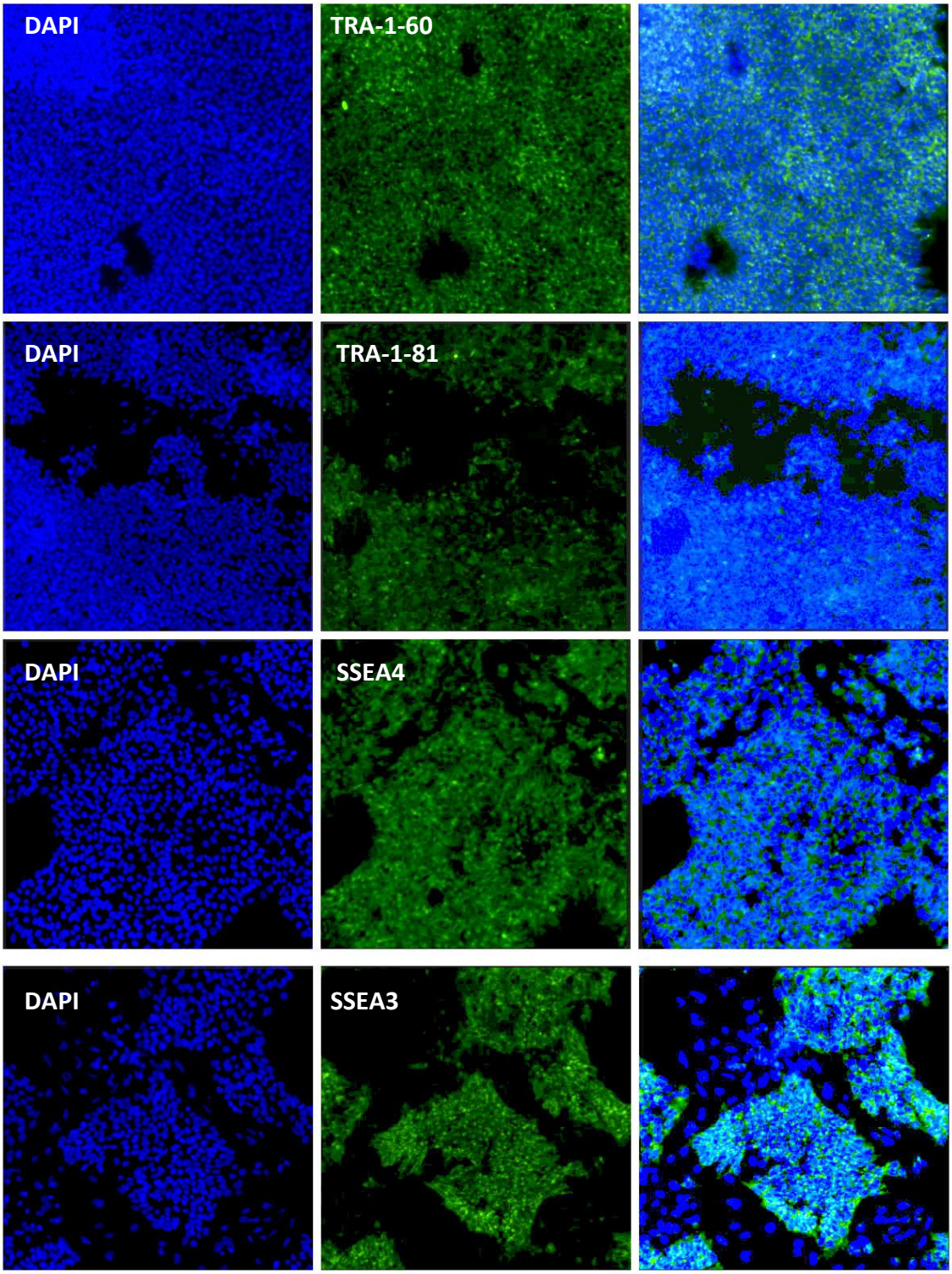

Figure 3.3-E: **Expression of surface protein markers of iPSC K2 by immunoflurosence staining.** Fluorescence microscope images for iPSC K2 after staining them for surface markers TRA-1-60, TRA-1-81, SSEA3, and SSEA4. Blue color of DAPI represent nuclear counter stain. Green color represents the specific staining of the intended markers. The stained cells were analyzed using the IX-81 fluorescent microscope (Olympus) with Cell^F software (Olympus).

3.1.3 Gene expression of pluripotencey makers by RT-PCR:

To test the pluripotency state of iPSC, we investigated the expression level of thepluripotency-associated genes: *DNMT3B, GABRB3, GDF3, LIN28, NANOG, POU5F1* and *TDGF1*using semi-quantitative PCR (RT-PCR). Analysis of cycle threshold (Ct) values of iPSC lines were determined and compared to their original fibroblast, fibro "S" used for iPSC (S1,S2,S3,S4,S5,S6) and fibro"K" for iPSC (K1,K2,K3,K4).Three technical replicates for each sample were performed to evaluate ΔCt mean. The results show that the ΔCt of iPSC lines for all the genes tested are significantly lower, compared with their original fibroblasts. These results indicate that we were able to successfully generate iPSC from fibroblasts (Figure 3.4).

Figure 3.4 :

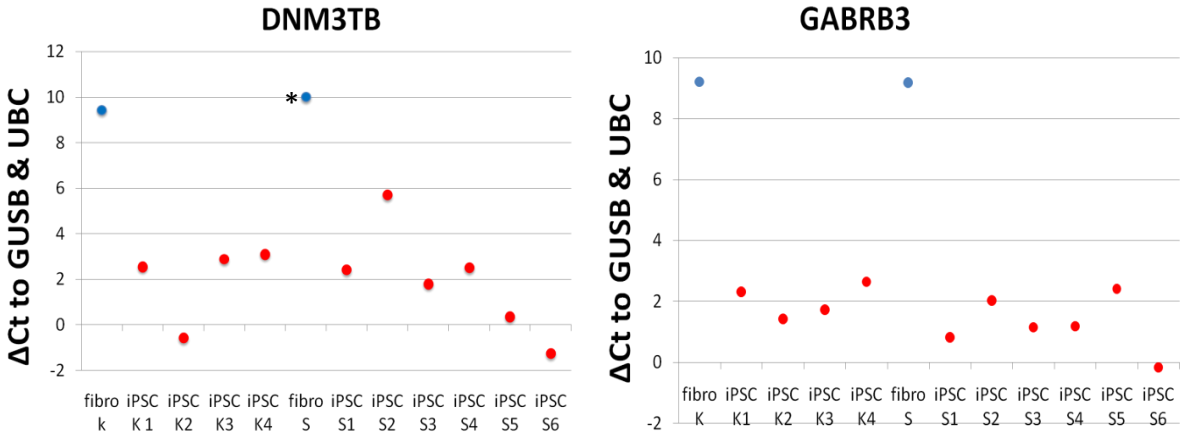

*ΔCt value of this fibroblast is arbitrarily set at 10, since no expression was observed.

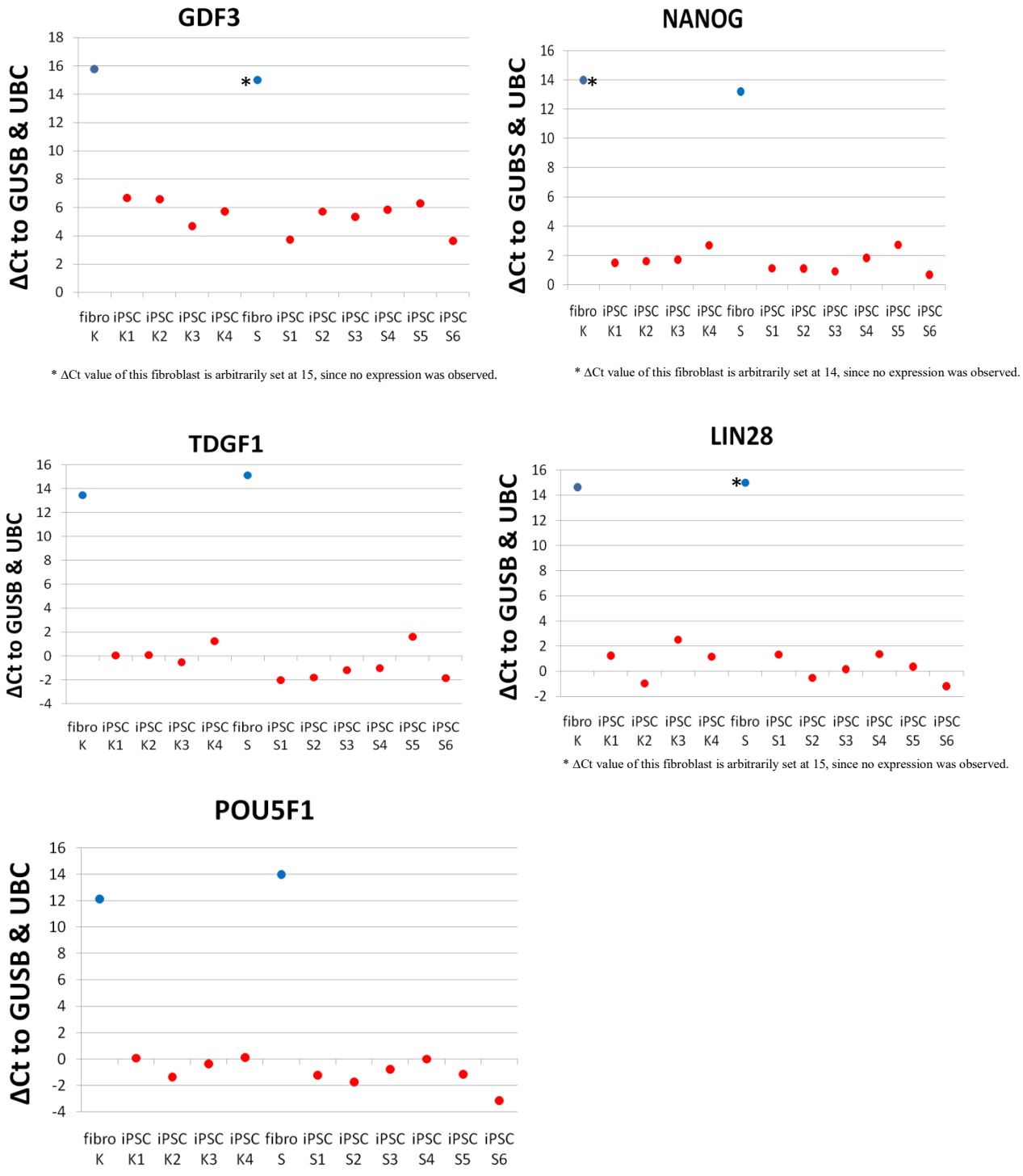

Figure 3.4: RT-PCR analysis of pluripotency marker genes. Representative figures showing the relative expression of the shown pluripotency genes in RNA extracted from for iPSC (K1,K2,K3,K4) derived from fibro "K" and iPSC (S1,S2,S3,S4,S5,S6) from fibro "S". Gene expression is measured as $\Delta Ct = Ct_{goi} - Ct_{ref}$ (where Ct -cycle threshold, goi – gene of interest , ref- reference gene). *GUSB* and *UBC* were used as

3.2 X-chromosome inactivation pattern of iPSC lines display skewing

As DNA methylation is one of differences between active and inactive X chromosome, and because it plays an important role for maintenance of its inactive state, we used HUMARA assay to investigate the XCI patterns of derived iPSC lines.First, to make sure that the technique is working properly, we digested a male sample. As shown in figure 3.5-A, before digestion, the male showed one peak at 274 bp. After adding *HapII*, this peak was gone. This result was expected since male X chromosome is active and not methylated (figure 3.5-A). For fibro "S", there are two peaks of the polymorphic *AR* locus located at 260 and 272 bp, there is a 12 bp (4 CTG) differences between the two X alleles (figure 3.5-B). Whereas in fibro "K" the size of the two peaks is: 266 *bp* and 275 *bp*, the differences between the two X alleles is 9 bp, 3 CTG repeats (figure 3.5-C). As expected in somatic cells, fibro "S" and fibro "K", we observed random pattern of XCI from ABI capillary electrophoresis results before transduction (figure 3.5-B,C), since the smaller peak was disappeared after digestion and the second one remained in the same height.

Examination of the methylation status at the *AR* locus showed skewing in our derived iPSC lines from fibro "S" and fibro "K". In all the derived iPSC from fibro "S" and fibro "K" the smaller peak was gone after adding *HapII* , therefore, the first peak is unmethylated (figure 3.5- B,C). Except in iPSC S4 the second peak was the unmethylated one. We can noting the skewing in the patterns from a notable change in the ratio between the two peaks after digestion, as one of them became higher than before digestion. Thus, this peak is methylated and generated from the inactive X.

Apart from the lines that were derived specifically for this project, we also analyzed seven iPSC lines that were previously derived from the same fibro "S" donor in the same lab. In

these lines, although we often observed a clear change in the ratio between the two peaks, we never observed a complete digestion for either one of the two peaks, which is indicative for random XCI (figure3.5-D).In Table 3.1, is an overview of the values of DNA methylation patterns for all cell lines (iPSC lines and fibroblast donors), before and after digestion.

Figure 3.5-A:

A. Male control pattern:

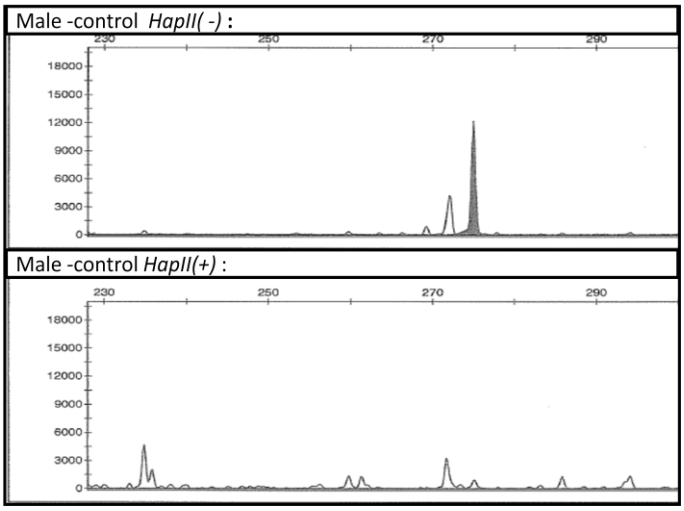

Figure 3.5-A: Methylation pattern analysis for male control cells. Results of methylation pattern analysis using fragment analysis of *AR* loci before *(HapII-)* and after (*HapII+)* digestion. The patterns for Male sample used as control for the digestion. The analysis was conducted using GeneMapper software (Applied Biosystems).

Figure 3.5-B:

B. Fibro “S” and iPSC “S1, S2, S3, S4, S5, S6” patterns:

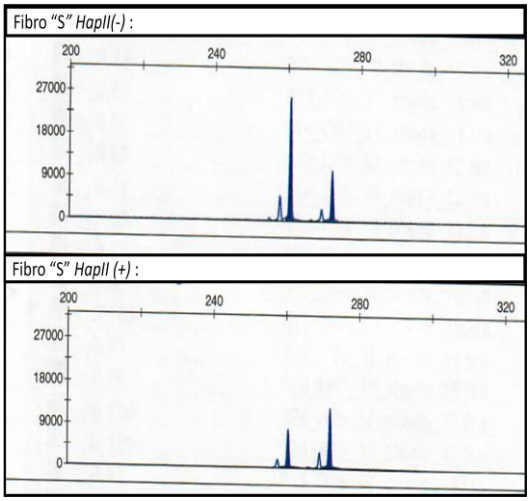

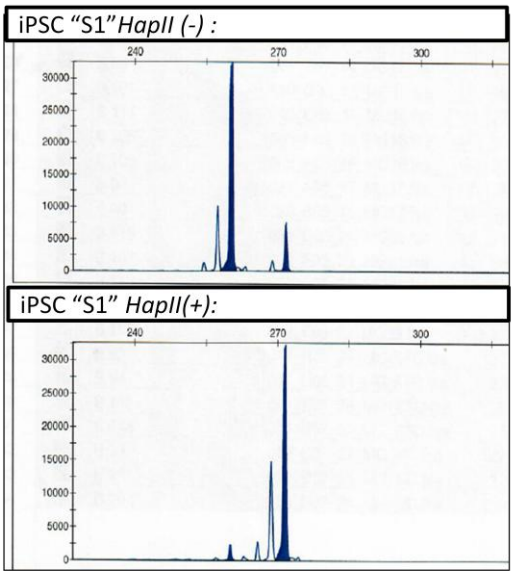

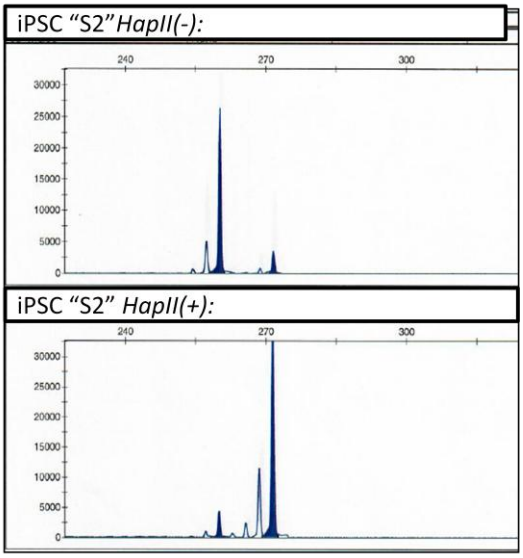

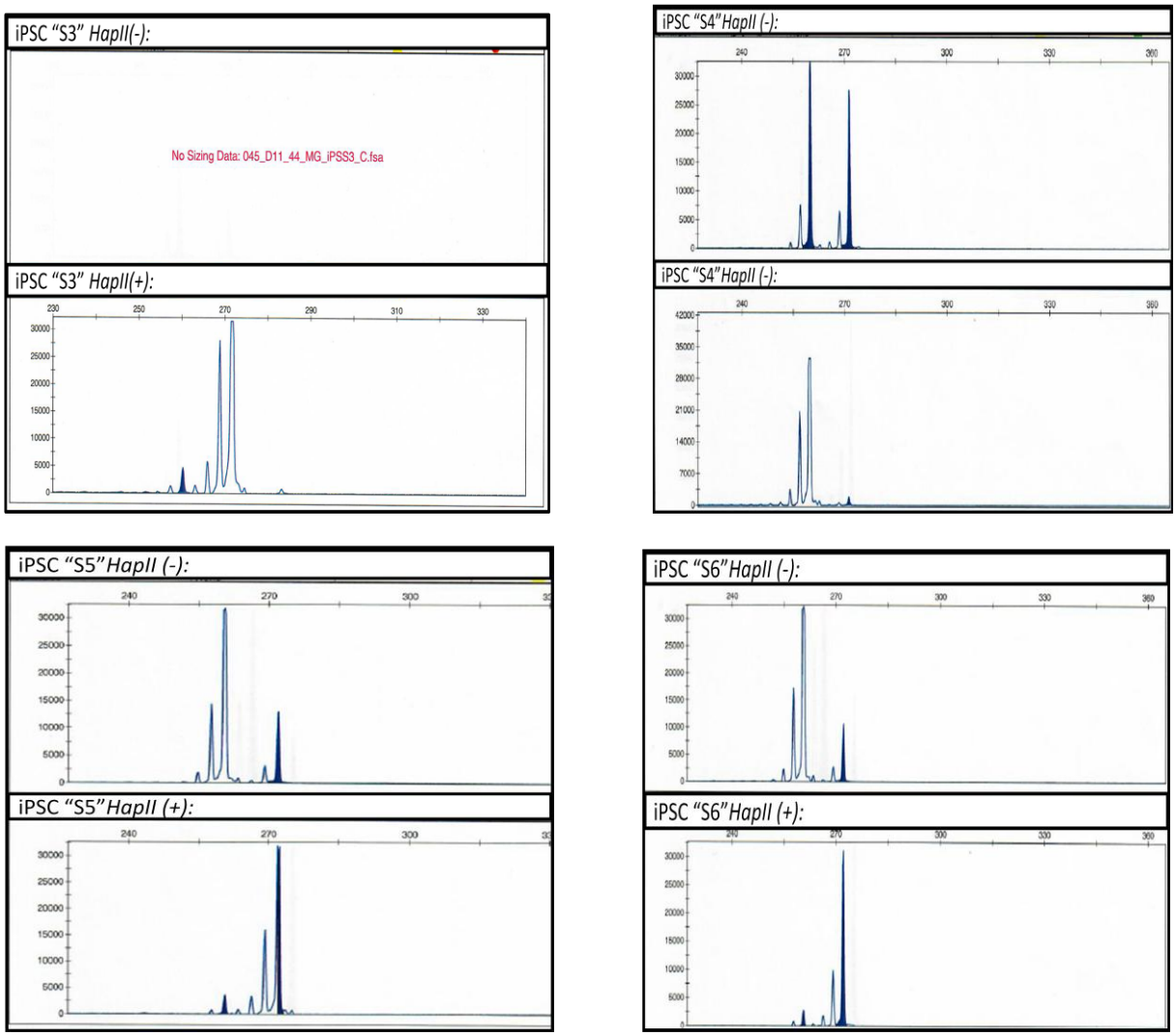

Figure 3.5-B: Methylation pattern analysis for fibro "S" and its derived iPSC (S1,S2,S3,S4,S5, and S6). Results of Methylation pattern analysis using fragment analysis of *AR* loci before *(HapII-)* and after (*HapII+)* digestion. The patterns for fibro "S" and its derived iPSC (S1, S2,S3,S4,S5 and S6) . The analysis was conducted using GeneMapper software (Applied Biosystems).

Figure 3.5-C :

C. Fibro “K” and iPSC (K1, K2,K3,K4)

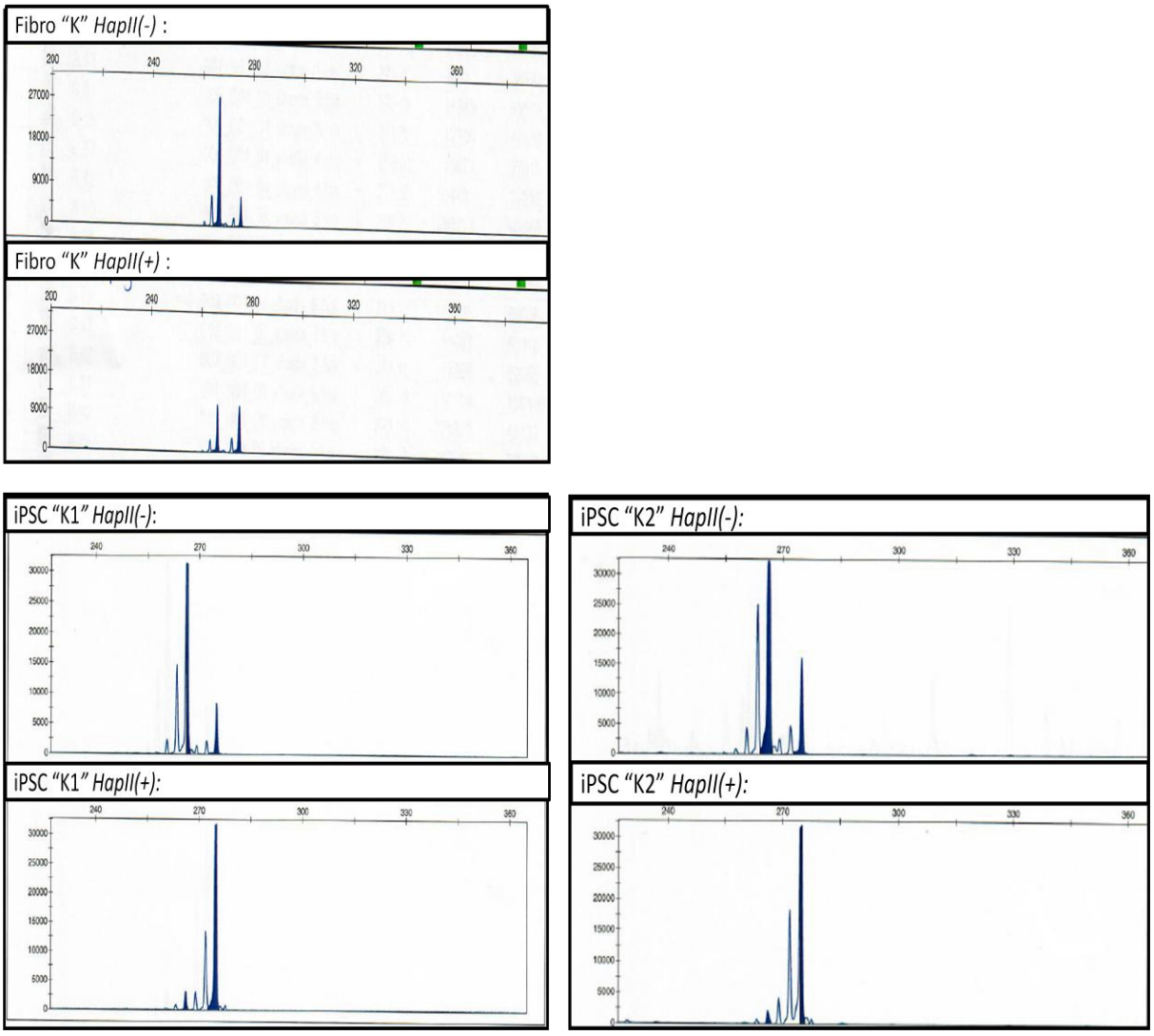

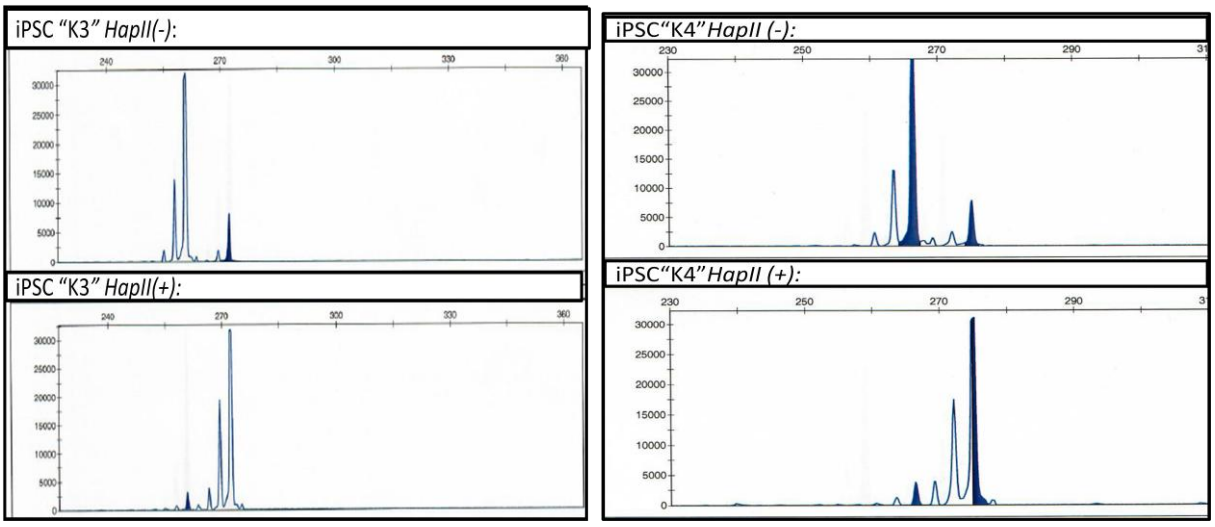

Figure 3.5-C: Methylation pattern analysis for Fibro "K" and its derived iPSC (K1,K2,K3, and K4). Results of Methylation pattern analysis using fragment analysis of *AR* loci before *(HapII-)* and after (*HapII+)* digestion. The patterns for fibro "K" and its derived iPSC (K1,K2,K3, and K4). The analysis was conducted using GeneMapper software (Applied Biosystems).

Figure 3.5-D:

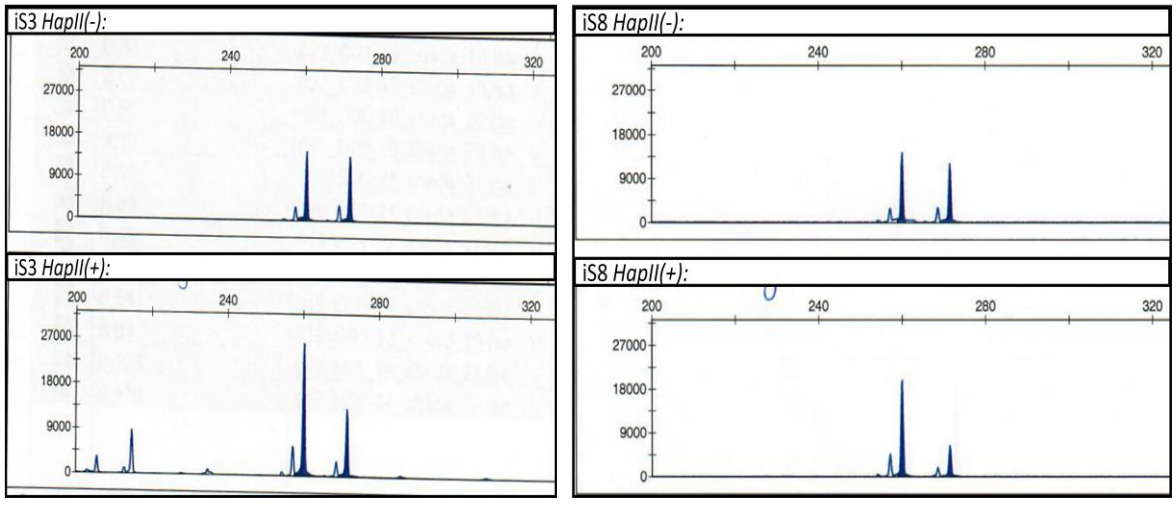

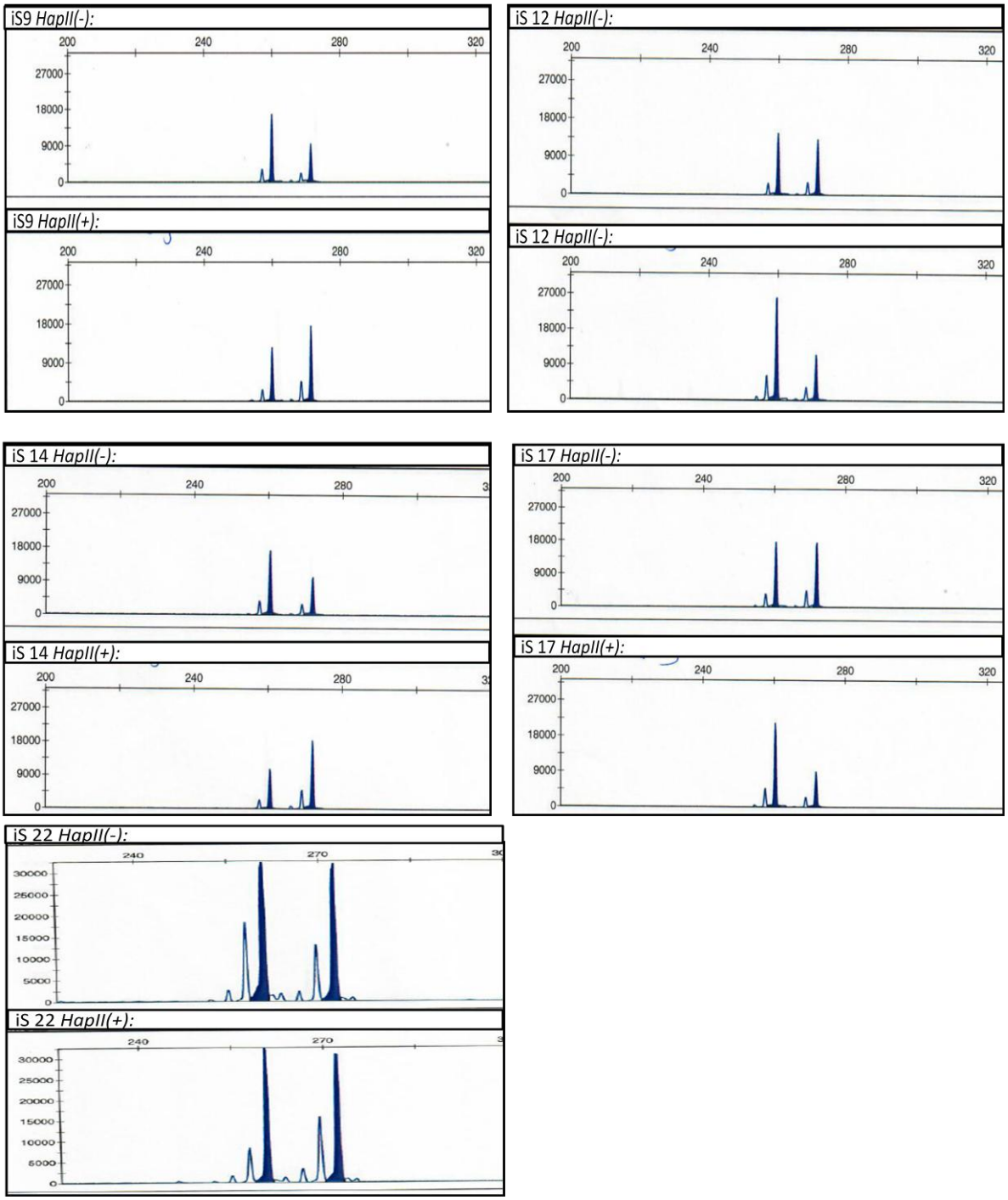

Figure 3.5-D: Methylation pattern analysis for iPSC lines derived before from fibro "S". Results of Methylation pattern analysis using fragment analysis of *AR* loci before *(HapII-)* and after (*HapII+)* digestion. The patterns for iPSC lines derived before from fibro "S" for a different project. The analysis was conducted using GeneMapper software (Applied Biosystems).

Table 3.1 Values of the peaks from DNA methylation patterns for the cell lines:

	HapII(-)				*HapII(+)*				
Cell line	**Peak 1 fragment**	**Size**	**Peak 2 fragment**	**Size**	**Peak 1 fragment**	**Size**	**Peak 2 fragment**	**Size**	**XCI pattern**
Male control	274	12173	NA	NA	274	1005	NA	NA	
Fibro "S"	260	16534	272	6871	260	30439	272	32060	Random
iPSC S1	260	32611	272	7649	260	2400	272	32397	skewing, 1st peak unmethylated
iPSC S2	260	26433	272	3585	260	4340	272	32534	skewing, 1st peak unmethylated
iPSC S3	260	NA	272	NA	260	<1000	272	32368	skewing, 1st peak unmethylated
iPSC S4	260	32595	272	27606	260	>35000	272	1843	skewing,2nd peak unmethylated
iPSC S5	260	>35000	272	13076	260	3690	272	31770	skewing, 1st peak unmethylated
iPSC S6	260	>35000	272	10705	260	2894	272	31205	skewing, 1st peak unmethylated
iS 3	260	14693	272	13915	260	26488	272	13606	doubt random/skewing
iS 8	260	14349	272	12100	260	19921	272	6443	doubt random/skewing
iS 9	260	16774	272	9621	260	12612	272	17625	doubt random/skewing
iS 12	260	14687	272	13286	260	26104	272	11623	doubt random/skewing
iS 14	260	17251	272	10072	260	10709	272	18497	doubt random/skewing
iS 17	260	17854	272	17675	260	21408	272	9110	doubt random/skewing
iS 22	260	32357	272	32021	260	32439	272	31025	doubt random/skewing
Fibro "K"	266	27595	275	6452	266	10994	275	10818	Random
K1	266	31509	275	8363	266	3133	275	31847	skewing, 1st peak unmethylated
K2	266	32289	275	16070	266	2255	275	31978	skewing, 1st peak unmethylated
K3	266	>35000	275	8172	266	3183	275	>35000	skewing, 1st peak unmethylated
K4	266	32247	275	7906	266	3820	275	30994	skewing, 1st peak unmethylated

Chapter Four

Discussion

In our work, we successfully generated ten iPSC lines from fibroblasts of two healthy female volunteers. Characterization, and investigation of X-chromosome inactivation patterns of hiPSC lines was evaluated. All of the derived iPSC showed pluripotencey state by expression of surface protein markers (TRA-1-81, TRA-1-60, SSEA3, and SSEA4) and pluripotencey gene markers*(DNMT3B, GABRB3, GDF3, TDGF1, LIN28, NANOG,*and*POU5F1).*Only S3 did not show positive immunofluresence stainingfor specific cell surface proteins. This might be because the cells are partially reprogrammed, since each cell line was generated from heterogeneous colony that need different time to be full reprogrammed. However, repeating immunofluoresence staining of membrane markers at later passage and check the differentiation capacity into the three germ layers, will give a real indication of the pluripotency state of this line.

The obtained lines were further used to investigate whether the XCI pattern in somatic cells has an influence upon iPSC reprogramming. According toDNA methyation analysis , anon-random XCI pattern was observed in the ten derived iPSC, suggesting that all hiPSC lineswere derived from a single fibroblast within the donor cell population. Based on Tchieu et al, this clonal hiPSC occurred without reactivation of Xi and the XCI in hiPSC line reflects that of the starting fibroblast (Tchieu, Kuoy et al. 2010).However, we cannot exclude that X chromosome reactivation happened during reprogramming, followed by non random inactivation. Bruck et

al. describe that female hiPSC, after initial X chromosome reactivation upon derivation, inactivate the same X chromosome that was inactive in the parental somatic cells they were derived from (Bruck, Yanuka, & Benvenisty, 2013).

Also, the fact that other iPSC lines that were derived before from one of the same donors (fibro "S") showed random XCI, may be suggestive for X chromosome reactivation. However, in this case, it would mean that the choice for which X chromosome to inactivate after initial reactivation is random, and the inactivation is thus not particularly occurring to the same X chromosome that was inactive in the somatic cell. It is still possible thought that these previously obtained lines were not clonally derived and the X reactivation did not happen. However, all of these possibilities should be further investigated, for example, examination if the reactivation has occurred can be tested by comparing the *XIST* state in the starting fibroblast and its derived iPSC (using allele-specific single-cell expression analysis).

The fact that we observed XCI skewing to the same X chromosome in our hiPSC (methylation of peak with size 272 in 5/6 S lines, methylation of peak with size 275 in 4/4 K lines), may suggest that(in)activation of a particular X chromosome confers a distinct advantage to these cells during cellular reprogramming or even during culture, as the passage number of the examined iPSC lines ranged from 3 to 7. However, in order to proof this, more experiments with these lines and with lines derived from other donors should be performed. An interesting experiment to investigate a possible culture advantage would be to perform competition experiments with S4 and one of the "S" lines with the opposite XCI pattern.

In order to examine if the culture advantage is driven by chromosomal aberration, the genetic content of the lines should be investigated. The types of genomic abnormalities that have been observed in hPSC range from whole chromosome to subchromosomal aberrations, including gene duplications and deletions and point mutations. Advantageous duplications or deletions will eventually take part when certain clones thrive during derivation and expanding of hPSC cultures. Also, when culture conditions are changed to drive specific forms of differentiation (Peterson & Loring, 2014). However, those abnormalities often confer a culture advantage and could confuse the hypothesis and experiments.

The nonrandom pattern of X chromosome in hiPSC has a critical impact for clinical application and disease modeling. For studies of X-linked diseases by using female hiPSC, it is very important to analyze which X chromosome is expressed. Isogenic cell populations with the nonrandom pattern would be preferable in gene therapy, because a mosaic population of cells expressing the mutant and wild-type allele from the female patient can be turned into a pluripotent, isogenic cell population that carries the mutant allele on the Xi in all cells and thus solely expresses the normal form of the gene (Tchieu et al., 2010) (Pomp, Dreesen et al., 2011). While random XCI is proposed for modeling X-linked diseasesand investigation of the disease phenotype. As derivation of iPSC from female with X-linked disorder could represent the normal cells by expressing the normal allele, and experimental mutant cells which express the mutant allele (Tchieu et al., 2010).

Recommendations:

For future work, more donors and iPSC lines should be examined to generalize the influence of X chromosome inactivation upon iPSC reprogramming. Also, it is would be helpful to

investigate XCI methylation related patterns for other polymorphic regions on X chromosome. Differentiation of iPSC lines is needed to test if the nonrandom pattern of XCI in undifferentiated hiPSC is maintained upon differentiation, and if the iPSC line could be applied in clinical applications. Also, looking at the differentiated progeny of iPSC will give insight into which class of hPSC it belongs (class I, II,III). If a mixed (random) population of XCIobtained after differentiation,the cells are belong to class I and reactivation occurs during reprogramming. The culture will shows homogenous population of X chromosome if they are belongs to class II or III, after differentiation (Dandulakis, Meganathan, Kroll, Bonni, & Constantino, 2016).

REFERENCES:

Briggs, S. F., & Pera, R. A. R. (2014). X chromosome inactivation: recent advances and a look forward. *Current opinion in genetics & development, 28*, 78-82.

Bruck, T., & Benvenisty, N. (2011). Meta-analysis of the heterogeneity of X chromosome inactivation in human pluripotent stem cells. *Stem cell research, 6*(2), 187-193.

Bruck, T., Yanuka, O., & Benvenisty, N. (2013). Human pluripotent stem cells with distinct X inactivation status show molecular and cellular differences controlled by the X-linked ELK-1 gene. *Cell reports, 4*(2), 262-270.

Consortium, I. H. G. S. (2001). Correction: Initial sequencing and analysis of the human genome. *Nature, 412*(6846), 565.

Dandulakis, M. G., Meganathan, K., Kroll, K. L., Bonni, A., & Constantino, J. N. (2016). Complexities of X chromosome inactivation status in female human induced pluripotent stem cells—a brief review and scientific update for autism research. *Journal of neurodevelopmental disorders, 8*(1), 22.

Disteche, C. M., & Berletch, J. B. (2015). X-chromosome inactivation and escape. *Journal of genetics, 94*(4), 591-599.

Ebert, A. D., Liang, P., & Wu, J. C. (2012). Induced pluripotent stem cells as a disease modeling and drug screening platform. *Journal of cardiovascular pharmacology, 60*(4), 408.

Geens, M., & Chuva De Sousa Lopes, S. M. (2017). X chromosome inactivation in human pluripotent stem cells as a model for human development: back to the drawing board? *Human reproduction update, 23*(5), 520-532.

Geens, M., Seriola, A., Barbé, L., Santalo, J., Veiga, A., Dée, K., . . . Spits, C. (2016). Female human pluripotent stem cells rapidly lose X chromosome inactivation marks and progress to a skewed methylation pattern during culture. *Molecular human reproduction, 22*(4), 285-298.

Hochedlinger, K., & Jaenisch, R. (2006). Nuclear reprogramming and pluripotency. *Nature, 441*(7097), 1061.

Kolios, G., & Moodley, Y. (2013). Introduction to stem cells and regenerative medicine. *Respiration, 85*(1), 3-10.

Lessing, D. M. C., & Lee, J. T. (2013). X chromosome inactivation and epigenetic responses to cellular reprogramming. *Annual review of genomics and human genetics, 14*, 85-110.

Lyon, M. F. (1961). Gene action in the X-chromosome of the mouse (Mus musculus L.). *Nature, 190*, 372-373.

Marchetto, M. C., Carromeu, C., Acab, A., Yu, D., Yeo, G. W., Mu, Y., . . . Muotri, A. R. (2010). A model for neural development and treatment of Rett syndrome using human induced pluripotent stem cells. *cell, 143*(4), 527-539.

Marone, M., Ritis, D. d., Bonanno, G., Mozzetti, S., Rutella, S., Scambia, G., & Pierelli, L. (2002). Cell cycle regulation in human hematopoietic stem cells: from isolation to activation. *Leukemia & lymphoma, 43*(3), 493-501.

Masaki, H., Ishikawa, T., Takahashi, S., Okumura, M., Sakai, N., Haga, M., . . . Shimada, F. (2008). Heterogeneity of pluripotent marker gene expression in colonies generated in human iPS cell induction culture. *Stem cell research, 1*(2), 105-115.

Merkle, F. T., & Eggan, K. (2013). Modeling human disease with pluripotent stem cells: from genome association to function. *Cell Stem Cell, 12*(6), 656-668.

Mitalipov, S., & Wolf, D. (2009). Totipotency, pluripotency and nuclear reprogramming *Engineering of stem cells* (pp. 185-199): Springer.

Ng, V. Y., & Choo, A. B. (2010). iPS and ES cells: do both roads lead to Rome. *Open Stem Cell J, 2*, 8-17.

Peterson, S. E., & Loring, J. F. (2014). Genomic instability in pluripotent stem cells: implications for clinical applications. *Journal of Biological Chemistry, 289*(8), 4578-4584.

Pomp, O., Dreesen, O., Leong, D. F. M., Meller-Pomp, O., Tan, T. T., Zhou, F., & Colman, A. (2011). Unexpected X chromosome skewing during culture and reprogramming of human somatic cells can be alleviated by exogenous telomerase. *Cell Stem Cell, 9*(2), 156-165.

Saha, K., & Jaenisch, R. (2009). Technical challenges in using human induced pluripotent stem cells to model disease. *Cell Stem Cell, 5*(6), 584-595.

Takahashi, K., Tanabe, K., Ohnuki, M., Narita, M., Ichisaka, T., Tomoda, K., & Yamanaka, S. (2007). Induction of pluripotent stem cells from adult human fibroblasts by defined factors. *cell, 131*(5), 861-872.

Takahashi, K., & Yamanaka, S. (2006). Induction of pluripotent stem cells from mouse embryonic and adult fibroblast cultures by defined factors. *cell, 126*(4), 663-676.

Tchieu, J., Kuoy, E., Chin, M. H., Trinh, H., Patterson, M., Sherman, S. P., . . . Zack, J. A. (2010). Female human iPSCs retain an inactive X chromosome. *Cell Stem Cell, 7*(3), 329-342.

Thomson, J. A., Itskovitz-Eldor, J., Shapiro, S. S., Waknitz, M. A., Swiergiel, J. J., Marshall, V. S., & Jones, J. M. (1998). Embryonic stem cell lines derived from human blastocysts. *science, 282*(5391), 1145-1147.

Tomoda, K., Takahashi, K., Leung, K., Okada, A., Narita, M., Yamada, N. A., . . . White, M. P. (2012). Derivation conditions impact X-inactivation status in female human induced pluripotent stem cells. *Cell Stem Cell, 11*(1), 91-99.

Van den Veyver, I. B. (2001). *Skewed X inactivation in X-linked disorders.* Paper presented at the Seminars in reproductive medicine.

Wutz, A. (2011). Gene silencing in X-chromosome inactivation: advances in understanding facultative heterochromatin formation. *Nature Reviews Genetics, 12*(8), 542.

Zhu, Z., & Huangfu, D. (2013). Human pluripotent stem cells: an emerging model in developmental biology. *Development, 140*(4), 705-717.

SUPPLEMENTARY TABLES

Supplementary Table 1 TaqMan gene expression assays for qRT-PCR

Gene symbol	TaqMan Assay
GABRB3	Hs00241459_m1
TDGF1	Hs02339499_g1
GDF3	Hs00220998_m1
GUSB	Hs99999908_m1
DNMT3B	Hs00171876_m1

Supplementary Table 2 The reverse, forward and the probe sequences for qRT-PCR

Gene symbol	Primer	Sequence
NANOG	Forward	5'-TGCAAATGTCTTCTGCTGGATG-3'
	Reverse	5'-TCCTGAATAAGCAGATCCATGGA-3'
	Probe	6-FAM-CAGAGACTGTCTCTCCTC-MGB)
UBC	Forward	5'-CGCAGCCGGATTTG-3
	Reverse	5'-TCAAGTGACGATACAGCGA-3'
	Probe	6-FAM-TCGCAGTTCTTGTTTGTG-MGB
GAPDH	Forward	5'-ATG GAA ATC CCA TCA CCA TCT T-3'
	Reverse	5'-CGC CCC ACT TGA TTT TGG -3'

	Probe	6-FAM-CAG GAG CGA GAT CC-MGB
LIN28	Forward	5’-CCC-CCA-GTG-GAT-GTC-TTT-GT-3’
	Reverse	5’-GCC-TCA-CCC-TCC-TTC-AAG-CT-3’
	Probe	6-FAM-CACCAGAGTAAGCTGCACATGGAAGGG-MGB
POU5F1	Forward	5’-GGACACCTGGCTTCGGATTT-3’
	Reverse	5’-CATCACCTCCACCACCTGG-3’
	Probe	6-FAM-GCCTTCTCGCCCCC-MGB

SUPPLEMENTARY FIGURES

Supplementary Figure 1:

A) iPSC S5

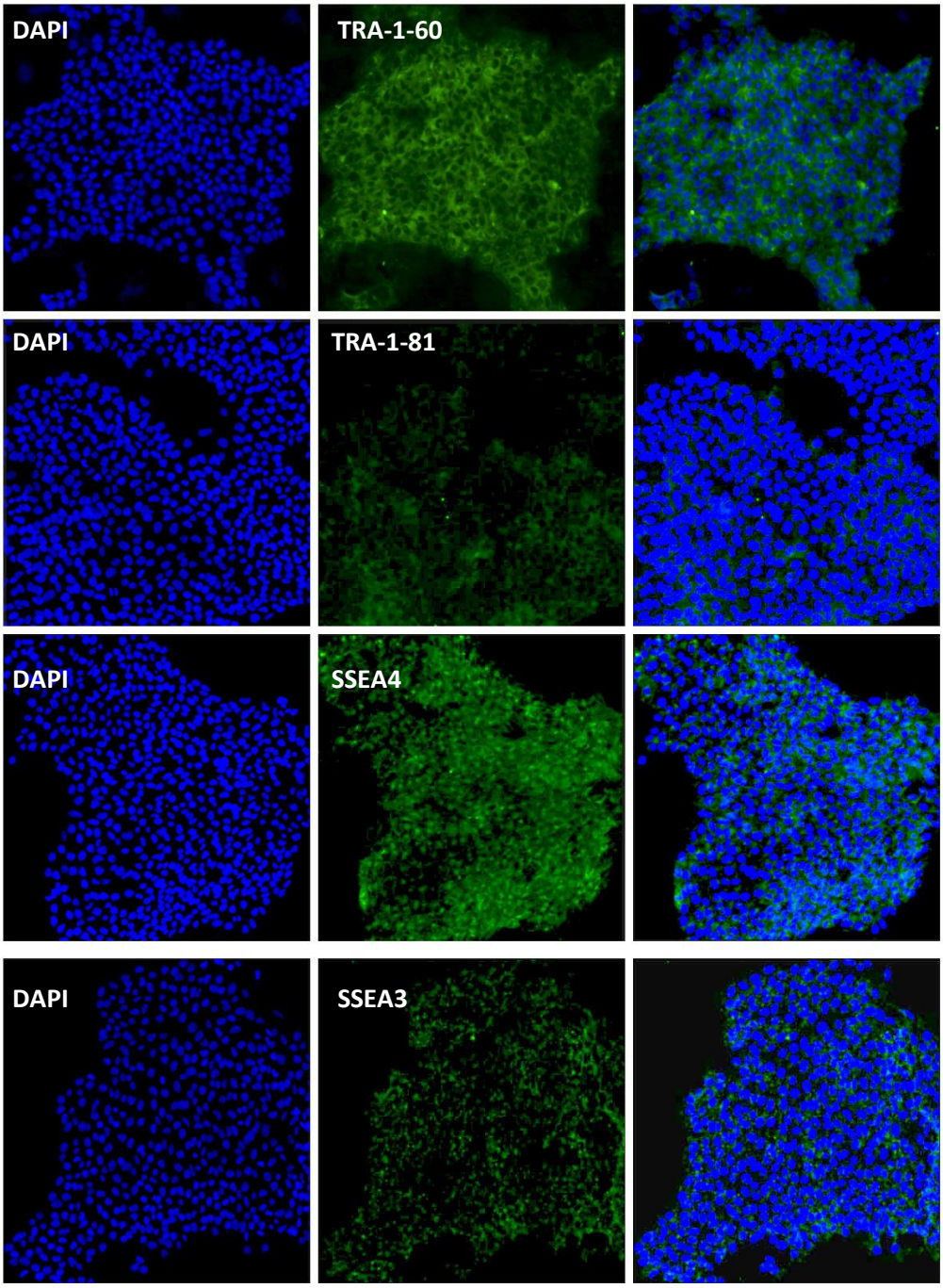

Supplementary Figure 1-A: Expression of surface protein markers of iPSC S5 by immunoflurosence staining. Fluorescence microscope images for iPSC S5 after staining them for surface markers TRA-1-60, TRA-1-81,SSEA3, and SSEA4. Blue color of DAPI represent nuclear counter stain. Green color represents the specific staining of the intended markers. The stained cells were analyzed using the IX-81 fluorescent microscope (Olympus) with Cell^F software (Olympus).

B) iPSC S4

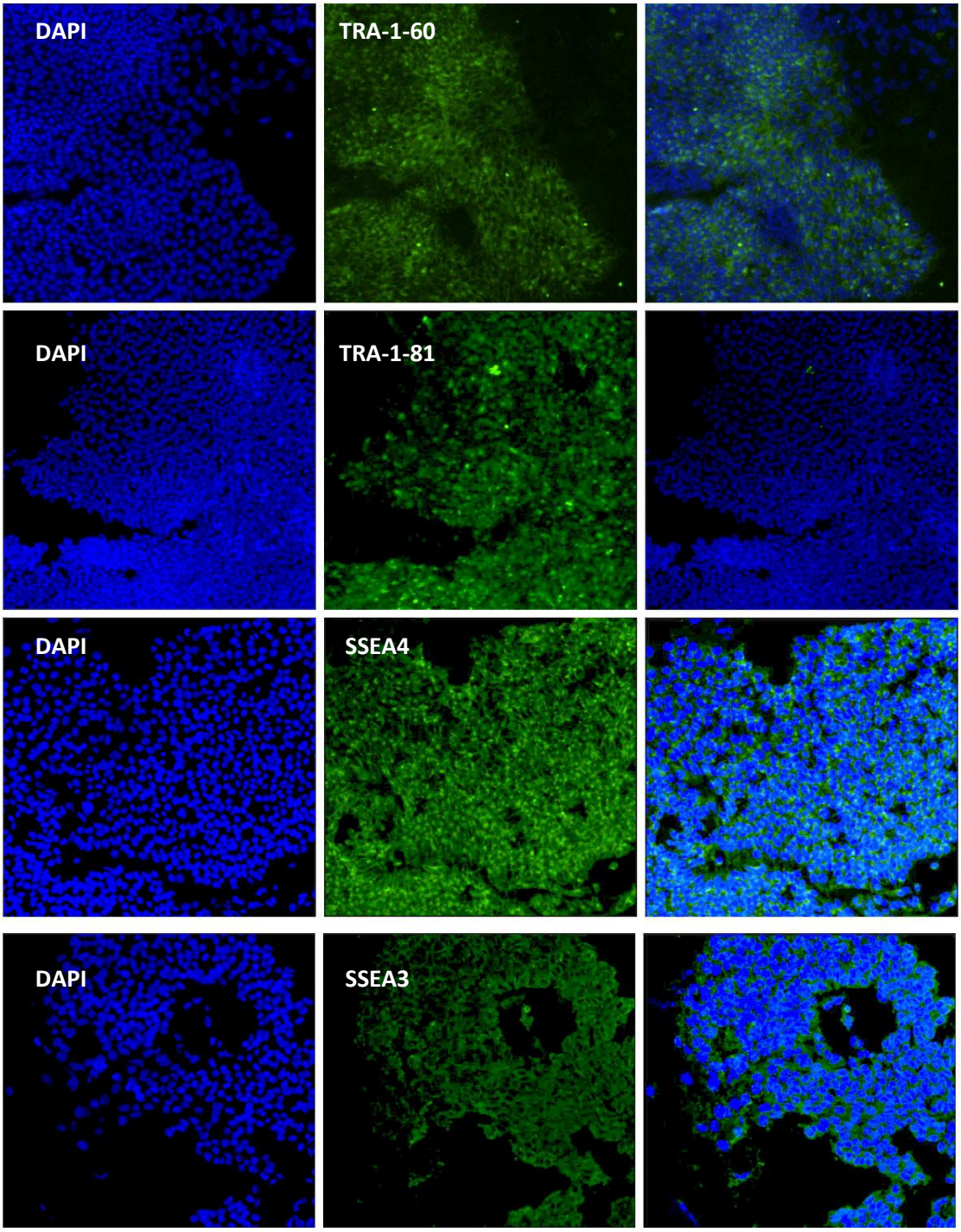

Supplementary Figure 1-B: Expression of surface protein markers of iPSC S4 by immunoflurosence staining. Fluorescence microscope images for iPSC S4 after staining them for surface markers TRA-1-60, TRA-1-81,SSEA3, and SSEA4. Blue color of DAPI represent nuclear counter stain. Green color represents the specific staining of the intended markers. The stained cells were analyzed using the IX-81 fluorescent microscope (Olympus) with Cell^F software (Olympus).

C) iPSC S6

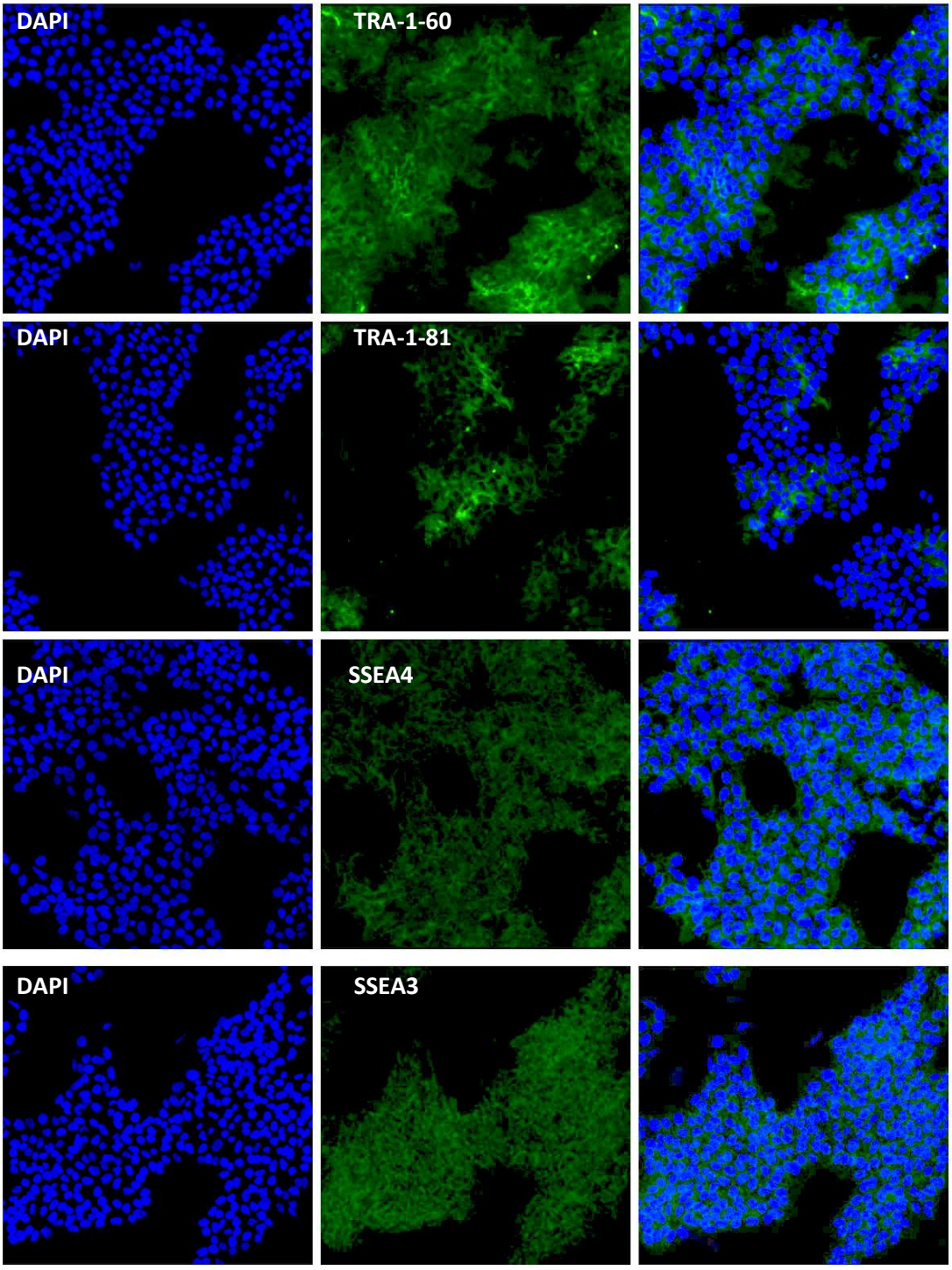

Supplementary Figure 1-C: Expression of surface protein markers of iPSC S6 by immunoflurosence staining. Fluorescence microscope images for iPSC S6 after staining them for surface markers TRA-1-60, TRA-1-81,SSEA3, and SSEA4. Blue color of DAPI represent nuclear counter stain. Green color represents the specific staining of the intended markers. The stained cells were analyzed using the IX-81 fluorescent microscope (Olympus) with Cell^F software (Olympus).

D) iPSC K3

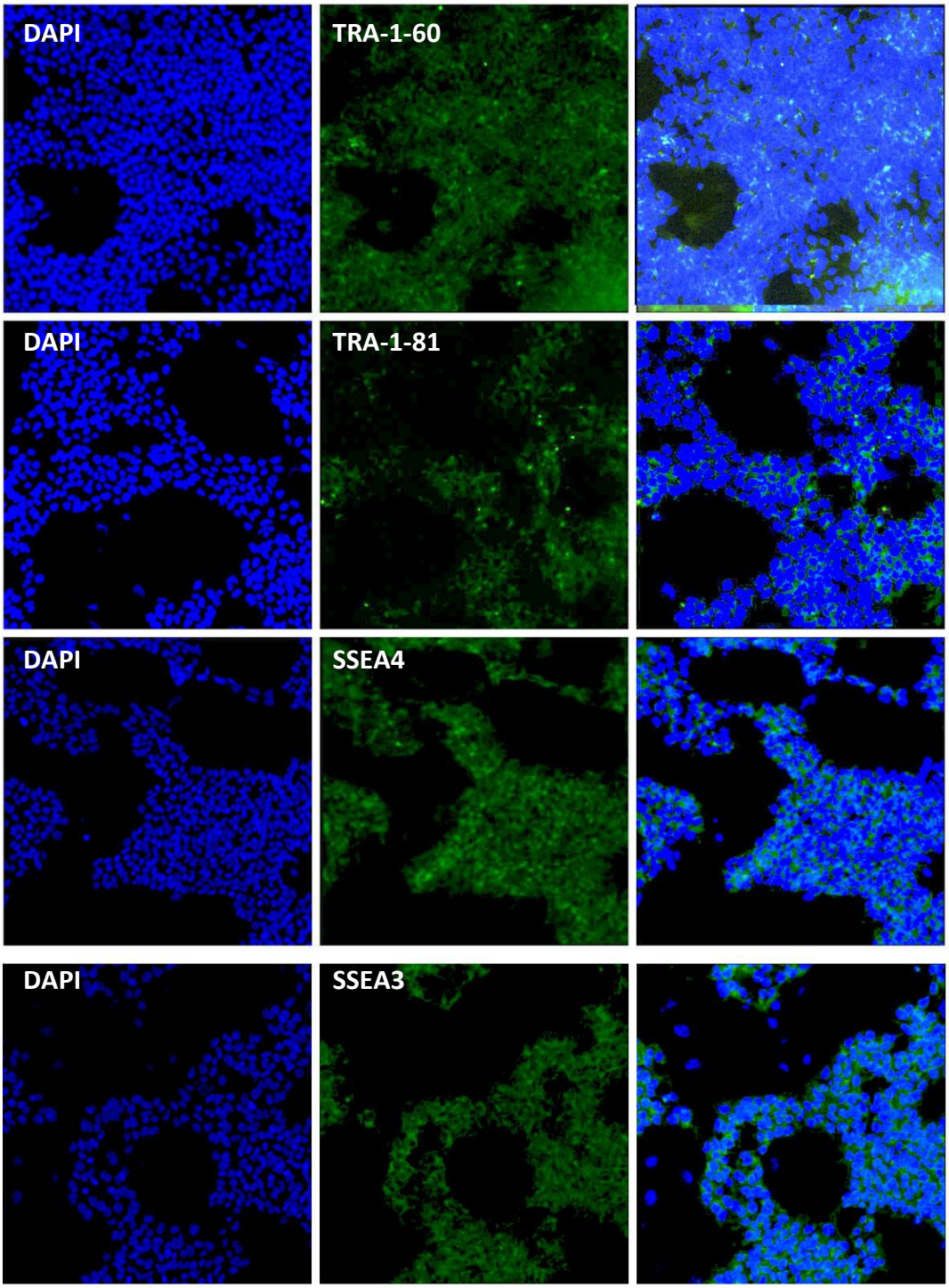

Supplementary Figure 1-D : Expression of surface protein markers of iPSC K3 by immunoflurosence staining. Fluorescence microscope images for iPSC K3 after staining them for surface markers TRA-1-60, TRA-1-81,SSEA3, and SSEA4. Blue color of DAPI represent nuclear counter stain. Green color represents the specific staining of the intended markers. The stained cells were analyzed using the IX-81 fluorescent microscope (Olympus) with Cell^F software (Olympus).

E) iPSC K4

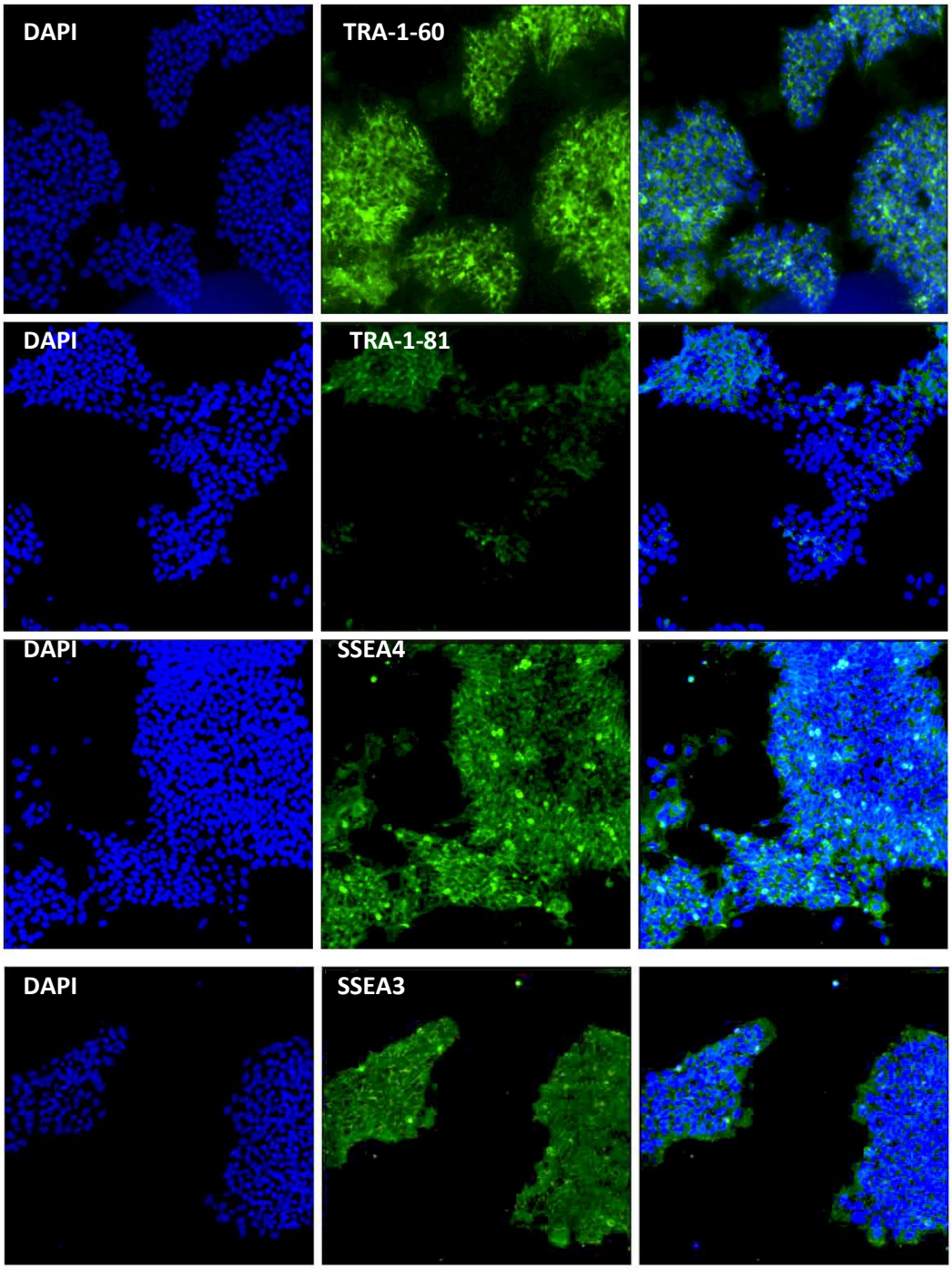

Supplementary Figure 1-E : Expression of surface protein markers of iPSC K4 by immunoflurosence staining. Fluorescence microscope images for iPSC K4 after staining them for surface markers TRA-1-60, TRA-1-81,SSEA3, and SSEA4. Blue color of DAPI represent nuclear counter stain. Green color represents the specific staining of the intended markers. The stained cells were analyzed using the IX-81 fluorescent microscope (Olympus) with Cell^F software (Olympus).

دراسة حالة تعطيل الكروموسوم X في الخلايا الجذعية المُستحثة لدى الإنسان

إعداد : شذى الإيمان صوالحة

بإشراف: الدكتور زيدون صلاح والدكتورة ميكا غننز.

الملخص:

خلال نمو وتطور الثدييات في المراحل الجنينية الأولى، تمر الإناث في عملية تسمى "تعطيل الكروموسوم X أو " XCI "حيث تقوم بتعطيل أحد الكروموسومين XX لدى الأُنثى لموازنة الفرق بين الجينات الناجمة عنهما بين الجنسين، من خلال إيقاف ترجمة الجينات المحمولة على هذا الكروموسوم ويتم اختيار الكروموسوم المراد تعطيله بشكل عشوائي.

استخدام الخلايا الجذعية ذات القدرة المتعددة (Pluripotent stem cells) في التطبيقات العلاجية ودراسة الأمراض على المستوى المخبري، يتطلب فهم عملية XCI وتأثيرها على إنتاج هذه الخلايا.

في هذه الدراسة قمنا في فحص إمكانية تأثير حالة الكروموسوم X في الخلايا الجسمية المتخصصة على الخلايا الجذعية المستحثة (induced pluripotent stem cells) المتولدة منها لدى الإنسان ، حيث قمنا بإنتاج 10 سلالات من الخلايا الجدعية المستحثة ، من خلال إعادة برمجة خلايا ليفية (fibroblasts) لأنثين سليمتين (Fibro "S", Fibro "K") ، حيث تم حقنهما بعوامل النسخ الأربعة (OCT4, SOX2, KLF4 and c-MYC) عن طريق الحقن الفيروسي.

وتم فحص حالة القدرة المتعددة للتخصص لدى هذه الخلايا من خلال فحص وجود البروتينات السطحية المميزة للخلايا المتعددة مثل (TRA-1-60 , TRA-1-81,SSEA3, SSEA4) من خلال عمل الصبغة المناعية المُشعة (immunofluorescenc staining).

وكذلك فحص إنتاج جينات تدل على الحالة المتعددة للخلايا مثل (DNMT3B, GABRB3, GDF3, TDGF1, NANOG, POU5F1, LIN28) ، باستخدام جهاز البلمرة المتسلسل (RT-PCR) .

إضافة إلى ذلك ، تم دراسة حالة XCI لهذه الخلايا والخلايا الليفية المانحة من خلال تحليل وجود مجموعة ميثل على الحمض النووي (DNA)، الذي تم من خلال تقنية (HUMARA assay) . وكذلك تم فحص حالة XCI في سلالات خلايا أخرى تم إنتاجها من قبل في نفس المختبر من إحدى الخلايا المانحة "Fibro S".

وقد أظهرت جميع الخلايا نتائج إيجابية لتشخيص حالة القدرة المتعددة للتخصص، تدل حصولنا على خلايا لها القدرة العالية على التخصص. أما بالنسبة لحالة الكروموسوم Xفي هذه الخلايا، فقد أظهرت النتائج وجود حالة غير عشوائية للكروموسوم X المُعَطل (non-random XCI) في العشر سلالات المنتجة من الخلايا المستحثة ، تدل أنه تم إنتاج أو توليد هذه الخلايا من نفس الخلية

الليفية، وكذلك وجود تأثير لكروموسوم X مُعين يعطي فائدة تُحسن من حياة باقي الخلايا خلال إعادة برمجتها أو خلال نموها. وسواء حدثت عملية إعادة تفعيل للكروموسوم المُعطل أم لم تحدث خلال إعادة برمجة الخلايا، فإنه يبدو أن نفس الكروموسوم X الذي كان مُعطلاً في الخلية الأم تم تعطيله في الخلايا المستحثة. لكن الخلايا المستحثة الأخرى التي تم إنتاجها سابقاً، أظهرت نتائج مغايرة، حيث وُجِدَ أنها تحمل جميعها عشوائية النموذج XCI مما يدل أنها قد مرت في عملية إعادة تفعيل للكروموسوم المعطل ويليها تعطيل عشوائي للكروموسوم قد لا يكون نفسه المعطل في الخلية الأم.

في النهاية، النتائج تُدل على وجود تأثير XCI على إنتاج وبرمجة الخلايا المستحثة لكن ما زلنا بحاجة إلى عمل المزيد من التجارب على خلايا مستحثة مختلفة ومن عدد أكبر من المانحين.